

NASA TECHNICAL
MEMORANDUM

NASA TM X-53790

October 7, 1968

NASA TM X-53790

GPO PRICE \$ _____

CFSTI PRICE(S) \$ _____

Hard copy (HC) 3.00

Microfiche (MF) .45

ff 653 July 65

LOW GRAVITY LIQUID-VAPOR INTERFACE SHAPES IN
AXISYMMETRIC CONTAINERS AND A
COMPUTER SOLUTION

Propulsion and Vehicle Engineering Laboratory

N 68-38059

FACILITY FORM 602

(ACCESSION NUMBER)

100

(PAGES)

TMX-53790
(NASA CR OR TMX OR AD NUMBER)

(THRU)

(CODE)

(CATEGORY)



NASA

George C. Marshall Space Flight Center
Marshall Space Flight Center, Alabama



TECHNICAL MEMORANDUM X-53790

LOW GRAVITY LIQUID-VAPOR INTERFACE
SHAPES IN AXISYMMETRIC CONTAINERS
AND A COMPUTER SOLUTION

By

Leon J. Hastings and Reginald Rutherford, III

George C. Marshall Space Flight Center
Marshall Space Flight Center, Alabama

ABSTRACT

A theoretical method for determining equilibrium interface configurations in axisymmetric containers of arbitrary shape was investigated. A single differential equation was derived from the principle of minimum surface and potential energy using the calculus of variations. This equation, in conjunction with boundary conditions dependent on container shape and contact angle, can be numerically solved for the desired surface profile using the Runge-Kutta iteration technique. The method imposes no significant limitations on contact angle or Bond number and is easily programmed for computer solutions. Representative theoretical results are presented concerning the influences of contact angle, Bond number, and container fill level on surface shapes. Also, theoretical results are compared with experimental data.

NASA - GEORGE C. MARSHALL SPACE FLIGHT CENTER

NASA-GEORGE C. MARSHALL SPACE FLIGHT CENTER

TECHNICAL MEMORANDUM X-53790

LOW GRAVITY LIQUID-VAPOR INTERFACE
SHAPES IN AXISYMMETRIC CONTAINERS
AND A COMPUTER SOLUTION

By

Leon J. Hastings and Reginald Rutherford, III

FLUID AND THERMAL SYSTEMS BRANCH
PROPULSION DIVISION
PROPULSION AND VEHICLE ENGINEERING LABORATORY
RESEARCH AND DEVELOPMENT OPERATIONS

TABLE OF CONTENTS

	Page
SUMMARY	1
I. INTRODUCTION	2
II. BASICS OF LIQUID-SOLID-VAPOR SYSTEMS	4
III. REVIEW OF PREVIOUS ANALYSES	7
IV. THEORETICAL ANALYSIS	15
A. Total Energy of a Capillary System	15
B. Principle of Minimum Energy	20
C. Application of Variational Principle	22
V. THEORETICAL RESULTS	29
A. Bond Number and Container Shape	29
B. Contact Angle	31
VI. EXPERIMENTAL VERIFICATION	45
VII. CONCLUSIONS	51
APPENDIX A - LIQUID-VAPOR-SOLID INTERFACES	53
APPENDIX B - BOUNDARY CONDITIONS DEPENDENT ON CONTAINER SHAPE	57
APPENDIX C - COMPUTER PROGRAM FOR DETERMINING INTERFACE SHAPE	64
REFERENCES	87

LIST OF ILLUSTRATIONS

Figure	Title	Page
1	Reference Coordinate System	8
2	Reference Coordinate System	16
3	Reference Polar Coordinate System	17
4	Low Gravity Zero Contact Angle Interface Shapes in Cylindrical Containers	33
5	Zero Contact Angle Interface Deviation from the Infinite Bond Number Level in a Cylinder	34
6	Zero Contact Angle Interface Shapes in Spherical Containers for Bond Number = 5	35
7	Zero Contact Angle Interface Shapes in Spherical Containers for Bond Number = 20	36
8	Zero Contact Angle Interface Shapes in Spherical Containers for Bond Number = 70	37
9	Zero Contact Angle Interface Shapes in Spherical Containers for Bond Number = 150	38
10	Zero Degree Contact Angle Interface Shapes in an Oblate Spheroid	39
11	Zero Degree Contact Angle Interface Shapes in a Prolate Spheroid	40
12	Effect of Contact Angle on Surface Shapes in a Cylinder	41
13	Contact Angle Influence on Surface Deviation from the Infinite Bond Number Position in a Cylinder	42
14	Effect of Contact Angle on Surface Shapes in a Sphere at Bond Number = 0	43
15	Effect of Contact Angle on Surface Shapes in a Sphere at Bond Number = 50	44
16	Experimental and Theoretical Interface Shapes in a Cylinder	48

LIST OF ILLUSTRATIONS (Concluded)

Figure	Title	Page
17	Experimental and Theoretical Interface Shapes in a Cylinder.....	49
18	Experimental and Theoretical Interface Shapes in a Cylinder.....	50
1A	Contact Angle Measurement	54
2A	Surface Tensions at a Liquid-Vapor-Solid Interface	55
1B	Geometry for Prolate and Oblate Spheroid Boundary Conditions	58
2B	Geometry for Boundary Conditions in a Cylinder	62

DEFINITION OF SYMBOLS

A	Area, ft^2
a	Local acceleration, ft/sec^2
b	Horizontal semi-axis of ellipse
B_N	Bond number based on R_o
C	$(y^2 + y'^2)$
E	Total energy, $\text{ft}\text{-lb}_f$
F	Integrand of integral to be minimized
G	Integrand of integral to be held constant
g_o	Dimension constant, $\text{lb}_m\text{ft}/\text{lb}_f\text{-sec}^2$
H	Bond number based on r_o
H'	Bond number based on r_c
K_o	Parameter related to curvature at interface centerpoint
k_o	Curvature at interface centerpoint
L	Arc length, ft
M	Mass, $\text{lb}_f\text{-sec}^2/\text{ft}$
P.E.	Potential energy, $\text{ft}\text{-lb}_f$
P	Pressure, lb_f/ft^2
Q	Heat, $\text{ft}\text{-lb}_f$
R	Container radius, ft
R_o	Characteristic container dimension, ft
r	Radius of curvature, ft
r_c	$\frac{\sigma l_v}{P_v - P_{l_o}}$
S.E.	Surface energy, $\text{ft}\text{-lb}_f$
S	Entropy, $\text{ft}\text{-lb}_f/^\circ\text{R}$
T	Temperature, $^\circ\text{R}$
U	Internal energy, $\text{ft}\text{-lb}_f$

DEFINITION OF SYMBOLS (Concluded)

V	Volume, ft ³
W	Work, ft - lb _f
X	Horizontal distance, ft
Y	Horizontal distance to container wall at (y, θ)
Y _B	Horizontal distance to container wall
y'	dy/d θ
y	Distance from origin to liquid surface
y _O	Distance from origin to low gravity surface centerpoint
y _g	Distance from origin to surface for Bond Number = ∞
Z	Vertical distance, ft
α	Contact angle, degrees
β	Empty fraction
θ	Angle measured from vertical axis to y, degrees
θ_1	θ at interface/container wall intersection, degrees
λ	Lagrange multiplier
ρ	Density, lb _f sec ² /ft ⁴
σ	Surface tension, lb _f /ft

SUBSCRIPTS

a	Acceleration
c	Capillary
l	Liquid
s	Solid
v	Vapor
w	Container wall

LOW GRAVITY LIQUID-VAPOR INTERFACE
SHAPES IN AXISYMMETRIC CONTAINERS
AND A COMPUTER SOLUTION

By

Leon J. Hastings and Reginald Rutherford, III

SUMMARY

The purpose of this study was to derive a convenient method for determining equilibrium liquid-vapor interface shapes in axisymmetric containers of arbitrary shape. Several legitimate methods for determining interface shapes were previously proposed by other investigators. In fact, the basic differential equation for computing interface profiles was presented by Bashforth and Adams in 1883. However, these solutions are either inconvenient to apply or are restricted to a certain range of boundary conditions.

A convenient form of the basic interface differential equation was derived from the familiar principle of minimum surface and potential energy using the calculus of variations. The use of a polar coordinate system eliminated the convergence difficulties encountered in the previous solutions. Also, the derivation enabled the incorporation of a Bond number based on a characteristic container dimension into the basic differential equation as opposed to a Bond number based on interface radius of curvature.

The basic differential equation and boundary conditions dependent on container shape were programmed for a GE235 computer so that surface shapes for any particular combination of Bond number, vapor volume, and contact angle can be determined. The computer solution utilizes the Runge-Kutta numerical technique and imposes no significant limitations on contact angle or Bond number.

Representative surface shapes were computed to determine the influence of contact angle, Bond number, and container fill level for three container shapes: cylindrical, spherical, and spheroidal. It was determined that, in a cylinder, the influence of Bond number on interface deformation is maximum between Bond numbers of two and twenty and becomes negligible for Bond numbers greater than approximately 200. In spherical or spheroidal containers, the empty fraction has a significant effect on the interface profile. Also, unlike the cylinder, a contact angle of 90 degrees does not assure negligible interface distortion in spherical or spheroidal containers. The limiting contact angle is that angle measured in the liquid between a horizontal plane corresponding to the infinite Bond number liquid level and the tangent to the container boundary.

The theoretical profiles were compared with experimental data, and exceptional agreement was obtained. In fact, if the actual contact angle is known, it is believed that the static equilibrium interface profiles can be computed with greater accuracy than they can be measured due to the distortion and reflection problems inherent in such experimental measurements.

I. INTRODUCTION

In environments devoid of any disturbances except that of a low acceleration or gravity, surface tension forces become comparable to those of gravity, and equilibrium liquid-vapor interface shapes may radically depart from the near flatness observed in normal gravity. This is especially true of the many liquids that exhibit wall contact angles at or near zero degrees. The problem of low gravity interface descriptions for various container shapes, liquids and acceleration levels is of especial interest to engineers responsible for the design of propellant control schemes for space vehicles and storage tankers that must operate for long periods of time in orbital environments, that is, under low gravity conditions.

The purpose of this study was to provide a general method that can be used to determine low gravity interface shapes for liquids in axisymmetric containers subjected to axial accelerations less than that of normal gravity. As demonstrated herein, a single differential equation, which is applicable to all containers that are symmetric about an axis parallel to the acceleration direction, can be derived from the principle of minimum potential and surface energy using the calculus of variations. This differential equation in conjunction with boundary conditions dependent on container shape and contact angle can be solved numerically for the desired interface shape using the Runge-Kutta iteration technique. Although the basic differential equation and its solution is applicable to all containers symmetric about the vertical axis, the following geometrical shapes were selected for analysis based on their practical significance in space vehicle applications: (a) cylindrical, (b) spherical, and (c) prolate and oblate spheroids. This theoretical method for interface determination was programmed for a GE 235 computer, and theoretical interface shapes were computed for a wide range of conditions. Since practically all known liquid propellants considered for space vehicle propulsion exhibit contact angles at or near zero degrees, interface configurations for fluids of zero contact angle are emphasized.

Also presented are experimental data concerning low gravity interface shapes that were obtained from a Lockheed Missiles and Space Company experimental program. Although the data are not extensive in scope, it is sufficient to substantiate the proposed theoretical techniques of interface shape determination.

II. BASICS OF LIQUID-SOLID-VAPOR SYSTEMS

A fundamental property of liquid surfaces is their tendency to contract to the smallest possible surface area for a given volume, i. e., a spherical surface. This property has been proven by thorough theoretical and experimental investigations which have been performed ever since the phenomena of capillarity was first noted by Leonardo da Vinci (Ref. 1)*. The properties of molecules in liquids can easily be used to account for this minimization of surface area. On the interior of the liquid, each molecule is surrounded by others on every side and is, therefore, subject to attraction in all directions. This, however, is not the case in the surface. Molecules in the surface are attracted inwards and to each side by neighboring molecules, but there is no outward attraction to balance the inward pull since the molecular density of the vapor is much less than that of the liquid. Hence, every surface molecule is subject to a strong inward attraction perpendicular to the surface. This inward attraction causes the surface molecules to move inwards more rapidly than others move outwards to replace them. The diminishing of molecules in the surface continues until the maximum number of molecules are in the interior, that is, until the surface is spherically shaped, subject to external conditions or forces acting on the liquid.

When external forces, such as gravity and those created by the presence of other materials, must be considered, the resulting liquid-vapor interface shapes are more complicated. Gravity forces always tend to minimize the potential energy associated with the mass of

* This reference contains an excellent summary of early works performed on capillary phenomena.

liquid affected by the liquid-vapor interface shape and, therefore, is an important factor in determining equilibrium interface shapes. In addition, another influencing factor that must be considered is the presence of a solid material and the molecular attraction between it and the liquid. If the molecules in the liquid are attracted by the solid (adhesive forces) more than by neighboring molecules in the liquid (cohesive forces), the liquid is said to "wet" the solid, that is, the liquid tends to spread on the solid surface. If the cohesive forces are greater than the adhesive forces, the liquid does not wet the solid surface.

Since surface energy is associated with a liquid-vapor interface and work must be done against the internal liquid molecules to extend the surface, a vast number of problems relating to the equilibrium position of surfaces can be solved if the magnitude of surface energy is known. To simplify the calculations, however, a hypothetical tension, which acts in all directions parallel to the surface, is substituted for the surface energy. This hypothetical tension is generally termed "surface tension." Surface tension has the same dimensions as surface energy per unit surface area and it must have the same numerical magnitude. Proof of this is relatively simple and is readily available in literature on physics of surfaces (a thermodynamic proof is contained in Ref. 2). Several references (see References 3 and 4) emphasize that the concept of liquid surfaces behaving like a stretched membrane must not be misconstrued, since surface energy is the fundamental liquid property and surface tension is merely its mathematical equivalent.

At any rate, the proper utilization of surface tension is very convenient. In systems involving liquid surfaces the equilibrium position can be acquired by totaling up the changes in surface energy of the various interfaces (liquid-solid, liquid-vapor, and solid-vapor) whose areas are altered by a displacement. However, if the surfaces are considered at the boundaries where each is pulling with the appropriate

"surface tension" on their boundaries, then the changes in liquid-solid and solid-vapor surface areas do not have to be calculated. Such an approach is taken in this report, which considers the effects of low gravity environments, container shapes, liquid "wettability"*, and liquid surface tension, on the equilibrium interface shape.

* The term "wettability" refers to the degree of solid-liquid attraction. The degree of wetting is usually measured in terms of "contact angle," which is explained in Appendix A.

III. REVIEW OF PREVIOUS ANALYSES

Several investigators have devoted considerable time to the evaluation of static equilibrium configurations of liquid-vapor systems in zero and low gravity environments. Most of their evaluations, however, apply only to containers of cylindrical shape (see for example References 5, 6, and 7). Only the works of Bashforth and Adams (Ref. 8); Reynolds, Saad, and Satterlee (Ref. 9); and Li (Ref. 10) can be applied to axisymmetric containers of arbitrary shape.

Undoubtedly, the most important early exploration of the subject was performed by Bashforth and Adams and is recorded in their book which was published in 1883. Bashforth and Adams were primarily concerned with the shape of liquid droplets on or suspended from a horizontal surface. Their results apply reasonably well to the present problem as demonstrated by Yeh and Hutton (Ref. 11) and Journey (Ref. 12).

Bashforth and Adams derived the governing differential equation beginning with the generally accepted relation for pressure difference across any curved liquid-vapor interface at a particular point

$$P_v - P_l = \sigma_{lv} \left(\frac{1}{r_1} + \frac{1}{r_2} \right) \quad (1)$$

where P_v and P_l are the pressures on the vapor and liquid side of the surface respectively, r_1 and r_2 are the principal radii of curvature of the surface at the point of interest, and σ_{lv} is the surface tension of the interface.

As shown in Figure 1, if P_{l0} is the interior pressure of the surface at its origin, then due to hydrostatic pressure variation

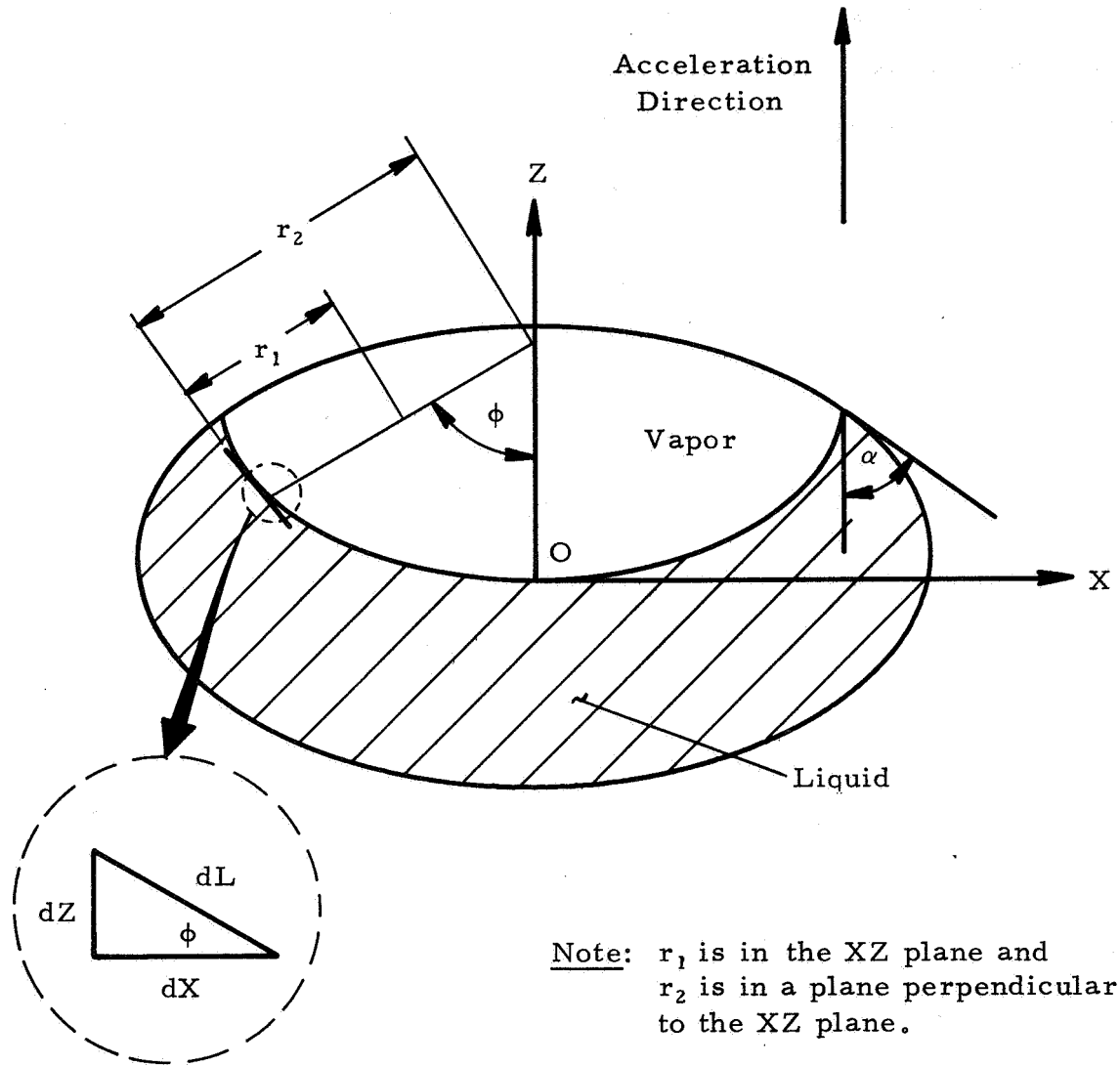


FIGURE 1. REFERENCE COORDINATE SYSTEM

$$P_l = P_{l0} - \rho_l a Z \quad (2)$$

where ρ_l is the liquid density and a is the local acceleration.
Also, at the origin

$$P_v - P_{l0} = \frac{2\sigma_{lv}}{r_0} \quad (3)$$

where $r_1 = r_2 = r_0$ in equation (1).

Using equation (3) and substituting for P_{l0} from equation (2),

$$P_v - P_l = \frac{2\sigma_{lv}}{r_0} + \rho_l a Z = \sigma_{lv} \left(\frac{1}{r_1} + \frac{1}{r_2} \right) \quad (4)$$

Let X be the horizontal and Z be the vertical coordinates of any point in a meridional section of the surface, r_1 the radius of curvature of the meridional section at that point, and ϕ the angle which the normal to the surface makes with the axis of revolution. Then, the length of the normal terminated by the axis (r_2) is $\frac{X}{\sin \phi}$, and equation (4) becomes

$$\frac{r_0}{r_1} + \frac{\sin \phi}{X/r_0} = 2 + H \left(\frac{Z}{r_0} \right) \quad (5)$$

where $H = \frac{\rho_l a r_0^2}{\sigma_{lv}}$ is a dimensionless number often termed the Bond number.

Another form of equation (5) can be easily derived. Since the expression for the radius of curvature of a line in the XZ plane is

$$r_1 = \frac{\left[1 + \left(\frac{dZ}{dX} \right)^2 \right]^{3/2}}{\frac{d^2 Z}{dX^2}}$$

and from Figure 1

$$\sin \phi = \frac{\frac{dZ}{dX}}{\left[1 + \left(\frac{dZ}{dX}\right)^2\right]^{1/2}}$$

then equation (5) is equivalent to

$$\frac{d^2Z}{dX^2} + \left[1 + \left(\frac{dZ}{dX}\right)^2\right] \frac{dZ}{XdX} = \left(\frac{2}{r_0} + \frac{HZ}{r_0^2}\right) \left[1 + \left(\frac{dZ}{dX}\right)^2\right]^{3/2} \quad (6a)$$

or

$$\frac{1}{X} \frac{d}{dX} \left\{ \frac{X \frac{dZ}{dX}}{\left[1 + \left(\frac{dZ}{dX}\right)^2\right]^{1/2}} \right\} = \frac{2}{r_0} + \frac{HZ}{r_0^2} \quad (6b)$$

These equations will be recognized in subsequent paragraphs as forms of the differential equation derived by other investigators using other approaches to the problem.

Equation (5) was solved by Bashforth and Adams using either the arc length L or ϕ as the independent variable. For example, if ϕ is taken as the independent variable, then upon integration of the equations

$$\frac{dX}{d\phi} = r_1 \cos \phi, \quad \frac{dZ}{d\phi} = r_1 \sin \phi \quad (7)$$

with use of the initial conditions at the origin

$$\phi = Z = 0; \quad r_1 = r_2 = r_0$$

equation (5) will yield r_1 as a function of the coordinates X and Z .

First, the form of the curve in the neighborhood of the origin can be found by developing r_1 and the coordinates X and Z in series of ascending powers of ϕ . Next, the coordinates for larger values of ϕ

can be obtained by step by step numerical integrations. Extensive numerical tables are presented in Reference 8 that give coordinates of surfaces for various values of H.

In present day space vehicle applications, it is desirable to base the interface shape on a Bond number in which a container dimension, such as tank radius, is the characteristic dimension. Bashforth and Adams' system can be converted to the desired Bond number system, but extensive interpolations are often required between tables in order to locate the proper liquid volume, contact angle (α), and Bond number combination. In addition, according to Yeh and Hutton's studies, Bashforth and Adam's tables contain a maximum Bond number (based on container radius) of about ten, so that for many applications their tables must be considerably extended.

Reynolds, et al obtained a modified but equivalent form of Bashforth and Adams' differential equation by performing a force balance on an infinitesimal annular ring cut from the meniscus. Using the coordinate system shown in Figure 1, a vertical force balance on an annular ring yields

$$\text{Capillary Force, } F_c = \text{Pressure Force, } F_p$$

or

$$d \left(2\pi X \sigma_{lv} \frac{dZ}{dL} \right) = (P_v - P_l) (2\pi X dX) \quad (8)$$

Substituting equation (2) for P_l ,

$$\sigma_{lv} \frac{d}{dL} \left(X \frac{dZ}{dL} \right) = \frac{XdX}{dL} (P_v - P_{l0} + \rho aZ) \quad (9)$$

Introducing the dimensionless quantities

$$x = \frac{X}{r_c} \quad z = \frac{Z}{r_c} \quad l = \frac{L}{r_c}$$

$$H' = \frac{\rho a r_c^2}{\sigma l v} \quad \text{where } r_c = \frac{\sigma l v}{(P_v - P_{l0})}$$

the final differential equation becomes

$$\frac{d}{dl} \left(x \frac{dz}{dl} \right) = x \frac{dx}{dl} (1 + H'z) \quad (10)$$

A second differential equation was obtained from the geometric condition

$$\left(\frac{dz}{dl} \right)^2 + \left(\frac{dx}{dl} \right)^2 = 1$$

which when differentiated, gives

$$\frac{dz}{dl} \frac{d^2 z}{dl^2} + \frac{dx}{dl} \frac{d^2 x}{dl^2} = 0 \quad (11)$$

Equations (10) and (11) form a pair that can be solved numerically.

The problem is treated as an initial value problem in which

$$x(0) = z(0) = z'(0) = 0$$

and

$$x'(0) = 1$$

Calculations of this type were performed for various values of H' (from 0 to 10) and contact angles. The calculations are similar to those of Bashforth and Adams and are subject to similar limitations.

In fact, it can be shown that equation (11) is a modified form of Bashforth and Adams' equation. Beginning with equation (9) and recalling that

$$P_v - P_{l0} = \frac{2\sigma l v}{r_0},$$

$$\frac{\rho_l aZ}{\sigma_{lv}} = \frac{HZ}{r_o^2},$$

and

$$dL = \left[1 + \left(\frac{dZ}{dX} \right)^2 \right]^{1/2} dX$$

then equation (9) becomes

$$\frac{1}{X} \frac{d}{dX} \left\{ \frac{X \frac{dZ}{dX}}{\left[1 + \left(\frac{dZ}{dX} \right)^2 \right]^{1/2}} \right\} = \frac{2}{r_o} + \frac{HZ}{r_o^2}$$

which is identical to equation (6b).

Using a still different approach, that is, the principle of minimum surface and potential energies and the calculus of variations, Ta Li* derived the interface differential equation

$$\frac{1}{X} \frac{d}{dX} \left\{ X \frac{dZ}{dX} \left[1 + \left(\frac{dZ}{dX} \right)^2 \right]^{-1/2} \right\} = \frac{HZ}{r_o^2} + \lambda$$

with

$$\lambda = \frac{2}{r_o} - \frac{H}{r_o^2} Z_o$$

where λ is a Lagrange multiplier; and at $Z = 0$

$$\frac{d^2Z}{dX^2} = \frac{1}{r_o}, \quad \frac{dZ}{dX} = 0, \quad \text{and} \quad Z = Z_o = 0$$

Then Li's final equation can be written

$$\frac{1}{X} \frac{d}{dX} \left\{ X \frac{dZ}{dX} \left[1 + \left(\frac{dZ}{dX} \right)^2 \right]^{-1/2} \right\} = \frac{HZ}{r_o^2} + \frac{2}{r_o}$$

which is identical to equation (6b).

* Li's derivation is not presented here since a similar procedure is used in the subsequent section of this report.

However, Li solved the differential equation through a transformation of variables and the introduction of a power series to give

$$\frac{Z}{r_0} = f(X)$$

Li obtained the first four terms of the expansion, and later Yeh and Hutton derived and used three additional terms of the expansion. However, the minimum contact angle for which Yeh and Hutton obtained satisfactory convergence was about 53 degrees. Yeh and Hutton concluded that Li's solution could not be used for contact angles at or near zero degrees, since the number of coefficients required for the series solution was a function of the cotangent of the contact angle, and therefore, an infinite number of coefficients was required as the contact angle approached zero.

In conclusion, it is noted that several approaches can be used to derive the basic differential equation for low gravity surface profiles. However, the independent variables chosen, the method of solution, and the coordinate system are important factors in obtaining numerical results for a wide range of conditions.

IV. THEORETICAL ANALYSIS

As related previously, Ta Li has proposed a general method of calculating low gravity liquid-vapor interface shapes in axisymmetric containers. His method appears to be legitimate but is unsuccessful in the many cases when the interface slope reaches or passes the vertical, i. e., curves back on itself. To avoid this difficulty, a polar coordinate system is proposed in the following sections. An integral equation is derived from energy considerations, and the calculus of variations is used to obtain a differential equation that can be solved numerically.

A. Total Energy of a Capillary System

Consider a container that is cylindrically symmetric and is partly filled with liquid. The total energy of this arrangement is the sum of surface and potential energies.

Total Energy = Surface Energy + Potential Energy

$$E = S.E. + P.E.$$

The surface energy is the sum of surface energy of three interfaces: liquid-vapor (lv), solid-vapor (sv), and solid-liquid (sl). Therefore,

$$S.E. = \sigma_{lv} A_{lv} + \sigma_{sv} A_{sv} + \sigma_{sl} A_{sl}$$

where σ is the surface tension and A is the area of the respective interfaces. Using the fact that the total area of the solid surface A_{total} is constant and the relation*

$$\sigma_{lv} \cos \alpha = \sigma_{sv} - \sigma_{sl}$$

where α is the wall/liquid-vapor interface contact angle, then

* Refer to the Appendix A for a discussion of this relation.

$$S.E. = \sigma_{lv} (A_{lv} - A_{sl} \cos \alpha) + \sigma_{sv} A_{total} \quad (12a)$$

or

$$S.E. = \sigma_{lv} (A_{lv} - A_{sl} \cos \alpha) + \text{Constant} \quad (12b)$$

Consider the coordinate system indicated in Figure 2. The independent variable is Z , the liquid-vapor surface is described by $X = X(Z)$; and the container boundary, which is axisymmetric about the Z axis, is described by $X_w = X_w(Z)$.

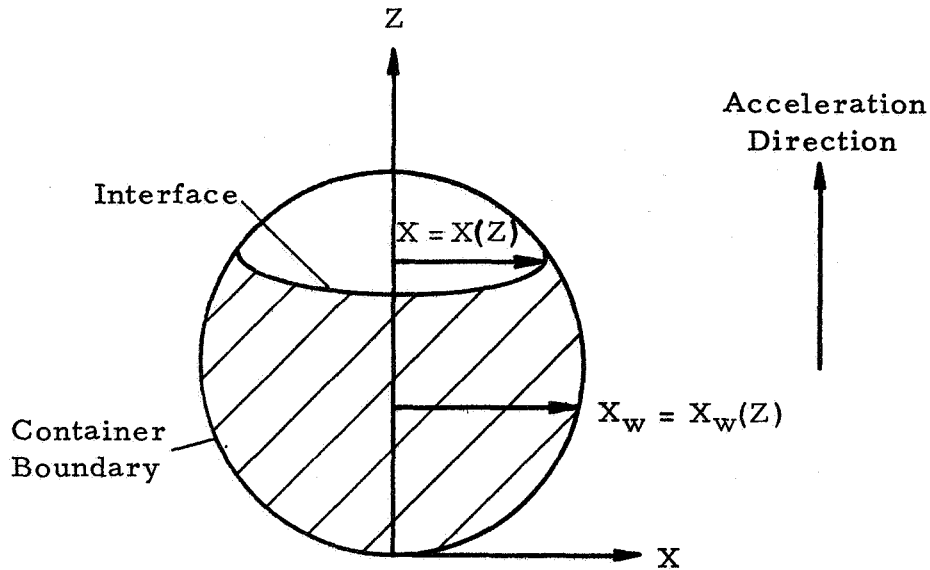


FIGURE 2. REFERENCE COORDINATE SYSTEM

The liquid-vapor interface surface area is

$$dA_{lv} = 2\pi X (\overline{dZ}^2 + \overline{dX}^2)^{1/2} \quad (13)$$

and the liquid volume (V_l), which is constant, is

$$dV_l = \pi(X_w^2 - X^2) dZ \quad (14)$$

Also, the potential energy of the liquid referenced to an arbitrary point on the liquid surface is

$$d(\text{P. E.}) = a(\rho_\ell - \rho_v) Z dV_\ell$$

or

$$d(\text{P. E.}) = \pi a \Delta\rho (X_w^2 - X^2) Z dZ \quad (15)$$

where: a = local acceleration of gravity

$\Delta\rho$ = liquid density - vapor density = $\rho_\ell - \rho_v$ (usually

$\Delta\rho = \rho_\ell$ for all practical purposes)

Now, consider a change to the coordinate system indicated in Figure 3.

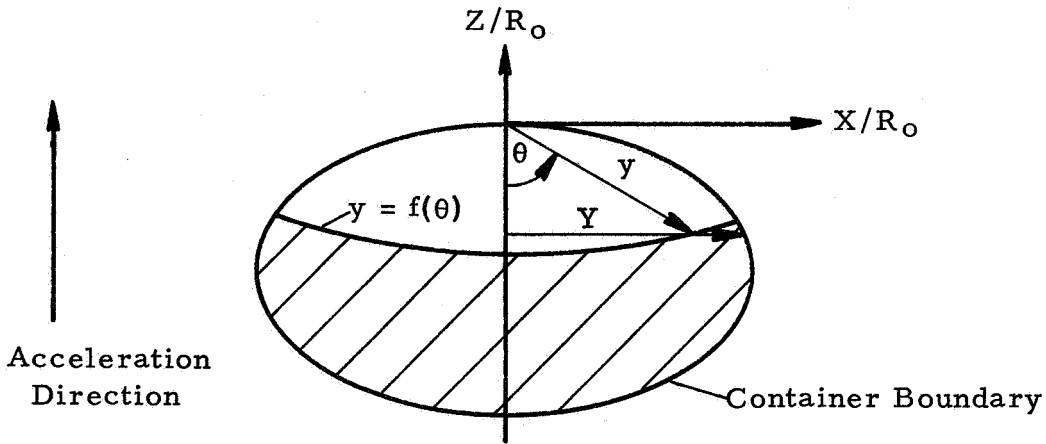


FIGURE 3. REFERENCE POLAR COORDINATE SYSTEM

The parameter y describes the liquid-vapor interface shape, and the angle θ , measured from the vertical to y , is the independent variable.

The coordinate transformation is

$$Z = - R_0 y \cos \theta \quad (16a)$$

$$X = R_0 y \sin \theta \quad (16b)$$

where R_0 is any convenient length parameter of the container. The

container boundary is now given by

$$Y = f(y, \theta) \quad (17)$$

where Y is the dimensionless radius of the container wall in a horizontal plane with the point (y, θ) .

In the new coordinate system, if relations (16) and (17) are substituted into equations (13), (14), and (15)

$$d A_{\ell v} = 2\pi R_o^2 y \sin \theta \left[y^2 + \left(\frac{dy}{d\theta} \right)^2 \right]^{1/2} d\theta \quad (18)$$

$$d V_{\ell} = \pi R_o^3 (Y^2 - y^2 \sin^2 \theta)(y \sin \theta - dy/d\theta \cos \theta) d\theta \quad (19)$$

$$d(\text{P.E.}) = -\pi a \Delta \rho R_o^4 y \cos \theta (Y^2 - y^2 \sin^2 \theta)(y \sin \theta - dy/d\theta \cos \theta) d\theta \quad (20)$$

Note that the total liquid volume must remain constant and from equation (19) is

$$V_{\ell} = \pi R_o^3 \int_0^{\theta_1} (Y^2 - y^2 \sin^2 \theta)(y \sin \theta - y' \cos \theta) d\theta + f(Z_o) \quad (21)$$

where $f(Z_o)$ is the volume of liquid below the horizontal plane at $\theta = 0$ and is, therefore, independent of the detailed form of interface shape. Using relations (12) and (18), a new relation can be derived for surface energy. Referring to Figure 3 and letting θ_1 be the final θ , i.e., θ measured at the interface/container wall intersection,

$$A_{\ell v} = 2\pi R_o^2 \int_0^{\theta_1} y \sin \theta (y^2 + y'^2)^{1/2} d\theta \quad (22)$$

Note: $y' = \frac{dy}{d\theta}$

Substituting equation (22) into (12)

$$\text{S. E.} = 2\pi R_o^2 \sigma_{lv} \left[\int_0^{\theta_1} y \sin \theta (y^2 + y'^2) d\theta - \frac{A_{sl} \cos \alpha}{2\pi R_o^2} \right]$$

+ Constant

However, A_{sl} is independent of the detailed form of $y(\theta)$, the interface shape, and is dependent only on θ_1 and the container boundary.

Therefore,

$$\frac{A_{sl}}{\pi R_o^2} = f(\theta_1)$$

and

$$\text{S. E.} = 2\pi \sigma_{lv} R_o^2 \left[\int_0^{\theta_1} y \sin \theta (y^2 + y'^2)^{1/2} d\theta - f(\theta_1) \cos \alpha \right] \quad (23)$$

+ Constant

From equation (20), the total potential energy is represented by

$$\text{P. E.} = -\pi a \Delta \rho R_o^4 \int_0^{\theta_1} y \cos \theta (Y^2 - y^2 \sin^2 \theta) (y \sin \theta - y' \cos \theta) d\theta \quad (24)$$

If a dimensionless parameter termed "Bond number," which is a ratio of "body forces" to "surface tension forces,"

$$B_N = \frac{\Delta \rho a R_o^2}{\sigma_{lv}}$$

is incorporated, then equation (24) becomes

$$\text{P. E.} = -\pi \sigma_{lv} B_N R_o^2 \int_0^{\theta_1} y \cos \theta (Y^2 - y^2 \sin^2 \theta) (y \sin \theta - y' \cos \theta) d\theta \quad (25)$$

By combining equations (23) and (25), the total energy is represented by

$$E = \pi \sigma_{lv} R_o^2 \left[2 \int_0^{\theta_1} y \sin \theta (y^2 + y'^2)^{1/2} d\theta - 2 f(\theta_1) \cos \alpha \right. \\ \left. - B_N \int_0^{\theta_1} y \cos \theta (Y^2 - y^2 \sin^2 \theta)(y \sin \theta - y' \cos \theta) d\theta \right] + \text{Constant} \quad (26)$$

In subsequent sections the expressions derived for total liquid volume, equation (21), and total energy, equation (26), will be used in conjunction with certain physical considerations to provide a basic equation for the equilibrium liquid-vapor interface profile. The physical considerations are that the total liquid volume must remain constant and that the principle of minimum energy must be satisfied.

B. Principle of Minimum Energy

Numerous investigators have observed through experimentation that the total energy, E , of a liquid-vapor-solid system such as the one under consideration, tends toward a minimum. The thermodynamics of such a capillary system can be used to explain this principle of minimum energy. Using equation (12b) the work required to extend the liquid-vapor interface is given by

$$d W_c = d(S.E.) = \sigma_{lv} dA_c$$

where $A_c = A_{lv} - A_{ls} \cos \alpha$.

The work performed against gravity when the capillary system's center of mass is moved upward a distance of dZ , is

$$d W_a = M dZ$$

Then the total reversible work done on a capillary system is

$$d W = \sigma_{lv} dA_c + M dZ \quad (27)$$

In a reversible or irreversible change of state, the entropy change, dS , is related to the energy transferred to the capillary system by

$$T dS = dU - dW \quad (28)$$

where U is the internal energy and T is the temperature.

Substituting equation (27) in equation (28)

$$T dS = dU - \sigma_{lv} dA_c - MadZ \quad (29)$$

The general criteria for neutral equilibrium of a system for all possible variations is

$$\Delta S)_E = \Delta E)_S = 0$$

and for stable equilibrium is

$$\Delta S)_E < 0 \quad \text{or} \quad \Delta E)_S > 0$$

where E is the stored system energy. Thus, in general, for all possible variations in the system for which

$$\Delta S)_E \leq 0 \quad \text{or} \quad \Delta E)_S \geq 0$$

a stable or neutral equilibrium state exists.

In this case, equation (29) represents the infinitesimal change between two equilibrium states. Consider changes at constant internal energy ($E = U$ in this analysis)

$$dS)_U = - \frac{\sigma_{lv} dA_c}{T} - \frac{MadZ}{T} \quad (30)$$

Then, if the initial state is in neutral or stable equilibrium and since T is always positive

$$dS)_U \leq 0 \quad \text{or} \quad \sigma_{lv} dA_c + MadZ \geq 0$$

and

$$dE \geq 0$$

Since the capillary system energy can only increase, the equilibrium state must be one of minimum energy, E.

Thus, the energy described by equation (26) must yield a minimum in order to satisfy the principle of minimum energy. As illustrated in the next section, this principle of minimum energy enables a convenient application of the calculus of variations.

C. Application of Variational Principle

In view of the aforementioned factors concerning the total energy and liquid volume of the system, it is necessary to minimize the total energy while keeping the liquid volume constant. Such a condition is known as an "isoperimetric problem" with a mobile upper limit (θ_1) in the calculus of variations. As shown by Li, it is convenient to use the calculus of variations to construct a function from Euler's relation (Ref. 13)

$$\frac{\partial(F + \lambda G)}{\partial y} - \frac{d}{d\theta} \left[\frac{\partial(F + \lambda G)}{\partial y'} \right] = 0 \quad (31)$$

where "F" and "G" are integrands of integrals to be minimized and held constant, respectively, and " λ " is a Lagrange multiplier. Therefore,

$$\begin{aligned} F &= F(y, \theta)* \\ &= 2y \sin \theta (y^2 + y'^2)^{1/2} \\ &\quad - B_N y \cos \theta (Y^2 - y^2 \sin^2 \theta)(y \sin \theta - y' \cos \theta) \end{aligned}$$

and

$$G = G(y, \theta)$$

* The term $f(\theta_1)$ is not included as a part of F because, as proven by Li, this only effect of the term is to assure the proper contact angle at the container boundary. Thus, this terminal condition is not satisfied for the time being.

$$G = (Y^2 - y^2 \sin^2 \theta)(y \sin \theta - y' \cos \theta)$$

Performing the indicated operations in equation (31),

$$\begin{aligned} \frac{\partial}{\partial y} (F + \lambda G) &= 2 \sin \theta (y^2 + y'^2)^{1/2} + 2y^2 \sin \theta (y^2 + y'^2)^{-1/2} \\ &\quad - B_N \cos \theta (Y^2 - y^2 \sin^2 \theta)(y \sin \theta - y' \cos \theta) \\ &\quad + \left(\frac{\partial Y^2}{\partial y} - 2y \sin^2 \theta \right) (\lambda - B_N y \cos \theta)(y \sin \theta - y' \cos \theta) \\ &\quad + \sin \theta (\lambda - B_N y \cos \theta)(Y^2 - y^2 \sin^2 \theta) \end{aligned} \quad (32)$$

and

$$\begin{aligned} \frac{d}{d\theta} \left[\frac{\partial(F + \lambda G)}{\partial y'} \right] &= \frac{d}{d\theta} \left[2y y' \sin \theta (y^2 + y'^2)^{-1/2} \right] \\ &\quad + \frac{d}{d\theta} \left[(B_N y \cos \theta - \lambda)(Y^2 - y^2 \sin^2 \theta) \cos \theta \right] \\ &= 2y y'' \sin \theta (y^2 + y'^2)^{-1/2} + 2y'^2 \sin \theta (y^2 + y'^2)^{-1/2} \\ &\quad - 2y y' \sin \theta (y y' + y' y'')(y^2 + y'^2)^{-3/2} \\ &\quad + 2y y' \cos \theta (y^2 + y'^2)^{-1/2} - (B_N y \cos \theta - \lambda)(Y^2 - y^2 \sin^2 \theta) \sin \theta \\ &\quad + (B_N y \cos \theta - \lambda) \left[\frac{d}{d\theta} (Y^2) - 2y y' \sin^2 \theta - 2y^2 \sin \theta \cos \theta \right] \cos \theta \\ &\quad + B_N (y' \cos \theta - y \sin \theta)(Y^2 - y^2 \sin^2 \theta) \cos \theta \end{aligned} \quad (33)$$

On combining relations (32) and (33) according to equation (31) and with considerable algebraic manipulation, it can be shown that:

$$\begin{aligned} 0 &= (2y^2 + 3y'^2 - yy'') C^{-3/2} - \frac{y' C^{-1/2} \cot \theta}{y} \\ &\quad + (\lambda - B_N y \cos \theta) \left[\frac{1}{2y} \left(\frac{\partial Y^2}{\partial y} + \frac{\partial Y^2}{\partial \theta} \frac{\cot \theta}{y} \right) - 1 \right] \end{aligned} \quad (34)$$

where $C = (y^2 + y'^2)$ for simplification.

On examining $\frac{\partial Y^2}{\partial y} + \frac{\cot \theta}{y} \frac{\partial Y^2}{\partial \theta}$ where $Y = f(Z)$ and

$$Z = f(y, \theta) = -R_0 y \cos \theta$$

Note that

$$\frac{\partial Y^2}{\partial y} = \frac{dY^2}{dZ} \frac{\partial Z}{\partial y} = -R_0 \cos \theta \frac{dY^2}{dZ}$$

$$\frac{\partial Y^2}{\partial \theta} = \frac{dY^2}{dZ} \frac{\partial Z}{\partial \theta} = +R_0 y \sin \theta \frac{dY^2}{dZ}$$

Hence,

$$\frac{\partial Y^2}{\partial y} + \frac{\cot \theta}{y} \frac{\partial Y^2}{\partial \theta} = 0 \quad (35)$$

This relation is very significant, for it means that container shape drops out of the differential equation (34). Incorporating equation (35) in equation (34) and solving for y''

$$y'' = \frac{2y^2 + 3y'^2}{y} - \frac{y' \cot \theta (y^2 + y'^2)}{y^2} + \frac{1}{y} (B_N y \cos \theta - \lambda)(y^2 + y'^2)^{3/2} \quad (36)$$

The undetermined multiplier λ can be solved for by treating the problem as an initial value problem in which the following "initial conditions" are prescribed

$$\begin{aligned} y(0) &= y_0 \\ y'(0) &= 0 \text{ (interface symmetry)} \\ y''(0) &= y_0 (1 - K_0) \end{aligned}$$

The initial value for $y''(0)$ can be derived using the equation for curvature of an arc at any particular point

$$k = \frac{y^2 + 2y'^2 - y y''}{(y^2 + y'^2)^{3/2}}$$

Substituting the conditions specified for $y(0)$ and $y'(0)$ and solving for $y''(0)$

$$y''(0) = y_0(-y_0 k_0)$$

or

$$y''(0) = y_0(1 - K_0)$$

where $K_0 = y_0 k_0$ and may be considered a parameter related to interface curvature at the point of symmetry. Therefore, by substituting the prescribed "initial conditions" in equation (36) and solving for λ

$$\lambda = \frac{2K_0}{y_0} + B_N y_0$$

Using this value for λ , the final form of the differential equation is obtained

$$y'' = \frac{2y^2 + 3y'^2}{y} - \frac{y'}{y^2} \cot \theta (y^2 + y'^2) + \frac{1}{y} \left[B_N (y \cos \theta - y_0) - \frac{2K_0}{y_0} \right] (y^2 + y'^2)^{3/2} \quad (37)$$

The validity of equation (37) can be checked at the two limiting conditions, namely, $B_N = 0$ and as B_N approaches infinity. At $B_N = 0$ (zero gravity), it has been experimentally verified by numerous investigators* that the surface of a totally wetting liquid will tend toward a shape of minimum surface area, that is, a sphere. Therefore, at $B_N = 0$ equation (37) must be satisfied by the equation for a circle, $y = y_0 \cos \theta$.

* See, for example, Reference 14.

Substitution of

$$y = y_0 \cos \theta$$

$$y' = -y_0 \sin \theta$$

$$K_0 = 1 - \frac{y''(0)}{y_0} = +2$$

in equation (37) gives

$$y'' = -y_0 \cos \theta$$

which verifies that $y = y_0 \cos \theta$ at $B_N = 0$.

As B_N approaches infinity the equation should become that for a horizontal line. That this occurs is easily verified by dividing equation (37) by B_N and taking the limit as B_N approaches infinity. In such a case, equation (37) becomes

$$0 = \frac{1}{y} (y \cos \theta - y_0)$$

or

$$y = \frac{y_0}{\cos \theta}$$

which is the equation for a horizontal line.

For values of B_N between the two end points, numerical solution of equation (37) is easily accomplished using the Runge-Kutta iteration technique (Ref. 15), which yields a dimensionless plot of the liquid-vapor interface for a given y_0 , K_0 , and B_N . However, the additional boundary conditions of contact angle, constant vapor (or liquid) volume, and container shape must be satisfied in order to obtain the desired interface shape. The equations for calculating these boundary conditions are all functions of container geometry and, therefore, constitute the only changes that must be considered when the container shape is modified. To illustrate the modifications that are required by a change in tank configuration, the equations for boundary conditions dependent

on tank shape are described in Appendix B for four shapes: spherical, prolate spheroid, oblate spheroid, and cylindrical.

Equation (37) and the boundary conditions described in Appendix B are programmed for a GE 235 computer so that the surface shape for any particular combination of Bond number, vapor volume, contact angle, and container shape can be determined. Basically, the calculation of a surface shape using the computer program consists of initiating the computation procedure with an initial set of conditions at the interface centerpoint and using the Runge-Kutta procedure until the calculated surface intersects the container wall. Whenever the surface reaches the container boundary, the boundary conditions of contact angle and vapor volume are checked. If these boundary conditions are not satisfied, appropriate changes in the initial set of conditions are selected by the computer and used to initiate the Runge-Kutta procedure again. Thus, the iteration procedure continues until all conditions are satisfied and the desired interface is yielded.

The computer program is described briefly in engineering terms in Appendix C. This information provides a better visualization of the relationships of the various parameters involved in the determination of an interface shape.

Thus, a differential equation (equation (37)) which enables the elimination of difficulties incurred in the application of previously derived interface differential equations (see Chapter III) has been formulated. Desirable features that have been incorporated in equation (37) include:

1. The Bond number, B_N , appearing in the differential equation is based on a characteristic container dimension rather than on the surface radius of curvature.

2. The polar coordinate system utilized eliminates the possibility of "double-valued" functions which can occur in other coordinate systems whenever the surface profile curves back on itself, that is,

whenever two values of Z occur for a given value of X . Thus, solutions are possible for zero contact angles and zero Bond numbers.

3. A computer solution of the differential equation is easily accomplished using the Runge-Kutta numerical technique. Bond number, contact angle, container shape, and fill level (except in the case of a cylinder) are the only necessary input.

Theoretical interface shapes for various conditions were determined using the computer program. The results are presented and discussed in the subsequent chapter.

V. THEORETICAL RESULTS

Low gravity interface shapes in spherical, prolate and oblate spheroidal, and cylindrical containers for a wide range of Bond numbers, fill levels, and contact angles were determined and are presented in Figures 4 through 15. However, since almost all known liquid propellants for space vehicle applications have contact angles near zero degrees, the presentation of interface shapes emphasizes shapes for zero degree contact angle fluids. A discussion of the influences of various parameters is contained in subsequent paragraphs.

A. Bond Number and Container Shapes

Figures 4 through 11 illustrate the effects of Bond number and tank configuration on surface shapes for zero degree contact angle fluids. As one would anticipate, the liquid-vapor interface shape approaches the shape observed in normal gravity as the Bond number increases. Some specific observations on the interface shapes calculated for each of the four container shapes analyzed are as follows:

1. Cylindrical Containers - Since container empty fraction has no influence on interface shape in a cylinder (provided the container top or bottom does not interfere with interface formation), Bond number is sufficient to prescribe interface shape for a given contact angle. Bond number as defined herein for a cylinder is

$$B_N = \frac{\rho a R^2}{\sigma_{lv}}$$

where the container radius, R , is the characteristic dimension. The vertical and horizontal coordinates of the interface shapes presented are, therefore, nondimensionalized with respect to container radius as follows

$$\frac{Z}{R} = \frac{\text{Vertical distance measured from Bond number} = \infty \text{ position}}{\text{Container radius}}$$

$$\frac{X}{R} = \frac{\text{Radial distance from container axis}}{\text{Container radius}}$$

Interface shapes for specific Bond numbers ranging from 0 to 200 are illustrated in Figure 4. However, the influence of Bond number on interface shape is best illustrated in Figure 5 where the vertical position of the low gravity interface at the two end points (at the container center and wall) are presented as a function of the Bond number from one to 1000. For Bond numbers less than two and greater than twenty, the interface shape begins to asymptotically approach maximum and zero deviation from a horizontal interface. Since a point of inflection occurs between Bond numbers of two and twenty, the Bond number influence on interface deformation is maximum in this region. Also, it is interesting to note that the interface distortion becomes very small or even negligible for Bond numbers greater than approximately 200.

If the interface shape is desired for a Bond number that is not presented, Figure 5 can be used to determine the position of the interface at its two end points. These two dimensions will aid in interpolating the interface data presented to find the required interface shape.

2. Spherical Containers - Since spherical containers are often considered for space vehicle applications, a rather extensive presentation of interface shapes is contained in Figures 6 through 9 for Bond numbers ranging from 5 to 150. The interface shape for the limiting case of Bond number equal zero was omitted because the interface merely assumes the shape of a sphere with a volume equal to the vapor volume in the container. The dimensionless parameters and symbols used in the figures presented are the same as those described for a cylinder.

The empty fraction has a very significant effect on the interface shape in a sphere for a given Bond number. This observation is evidenced by comparing the low gravity interface shapes for normal gravity liquid levels in the upper half of the container with those in the

lower half. The interface shapes in the lower half have significantly less curvature than those in the upper half because the interface must bend less to become tangent to the container wall and satisfy the zero degree contact angle condition.

3. Oblate and Prolate Spheroids - In cryogenic space vehicle applications, particularly liquid hydrogen (fuel)/liquid oxygen (oxidizer) systems, the oxidizer tank is usually an oblate spheroid or some modification thereof. As a typical spheroid, the oxidizer tank shape used on the Centaur space vehicle was chosen for analysis (1 by 1.38 ellipse). Interface shapes for four different fill levels and Bond numbers of 5, 20, 50, and 100 are shown in Figures 10 and 11. The dimensionless parameters used are the same as those for a sphere except that the characteristic length parameter, R_o , is one-half the vertical height of the spheroid. The selection of vertical height instead of container width as the characteristic dimension was necessary to simplify the integration of spheroidal shapes in the computer program. However, whether width or length is used in the Bond number is somewhat arbitrary as long as care is taken to maintain consistency when the influence of Bond number is discussed.

Examination of the interface shapes presented discloses that the interface characteristics are a combination of those noted for cylindrical and spherical containers. As one would probably anticipate, in addition to the effects of Bond number, contact angle, and empty fraction, the ratio of major axis to minor axis must be considered a very significant parameter when determining interface shapes in spheroidal containers.

B. Contact Angle

As mentioned previously, most liquid propellants considered for space applications seem to exhibit zero or near zero degree contact angles on solid materials. However, to illustrate the effect of contact

angle, representative interface shapes for contact angles from 5 to 90 degrees are presented in Figures 12 through 15 for cylindrical and spherical containers.

1. Cylindrical Containers - Figure 12 illustrates the effect of contact angle on interface profile for Bond numbers of 0 and 50; and as one would expect, the influence of contact angle decreases with increasing Bond number. The influence of contact angle is best demonstrated in Figure 13, where the interface rise above the infinite Bond number liquid level versus Bond number for various contact angles is presented. For example, examination of this figure reveals that the difference between surface shapes with 0 and 5 degree contact angles becomes almost negligible near a Bond number of 100.

2. Spherical Containers - High contact angle surface profiles are presented for three fill levels and Bond numbers of 0 and 50 in Figures 14 and 15. Unlike the cylinder, a contact angle of 90 degrees does not assure negligible interface distortion at all Bond numbers. The limiting contact angle in all container shapes is that angle measured in the liquid between a horizontal plane corresponding to the infinite Bond number liquid level and the tangent to the container boundary. Hence, in all vessels with curved boundaries, this limiting angle is dependent on fill level. It is not surprising, therefore, that for the fill level near the bottom of the sphere, the interface becomes flat for all Bond numbers when the contact angle is equal to 54 degrees. At the fill level near the top of the sphere a contact angle of about 143 degrees is required before Bond number no longer affects the surface shape.

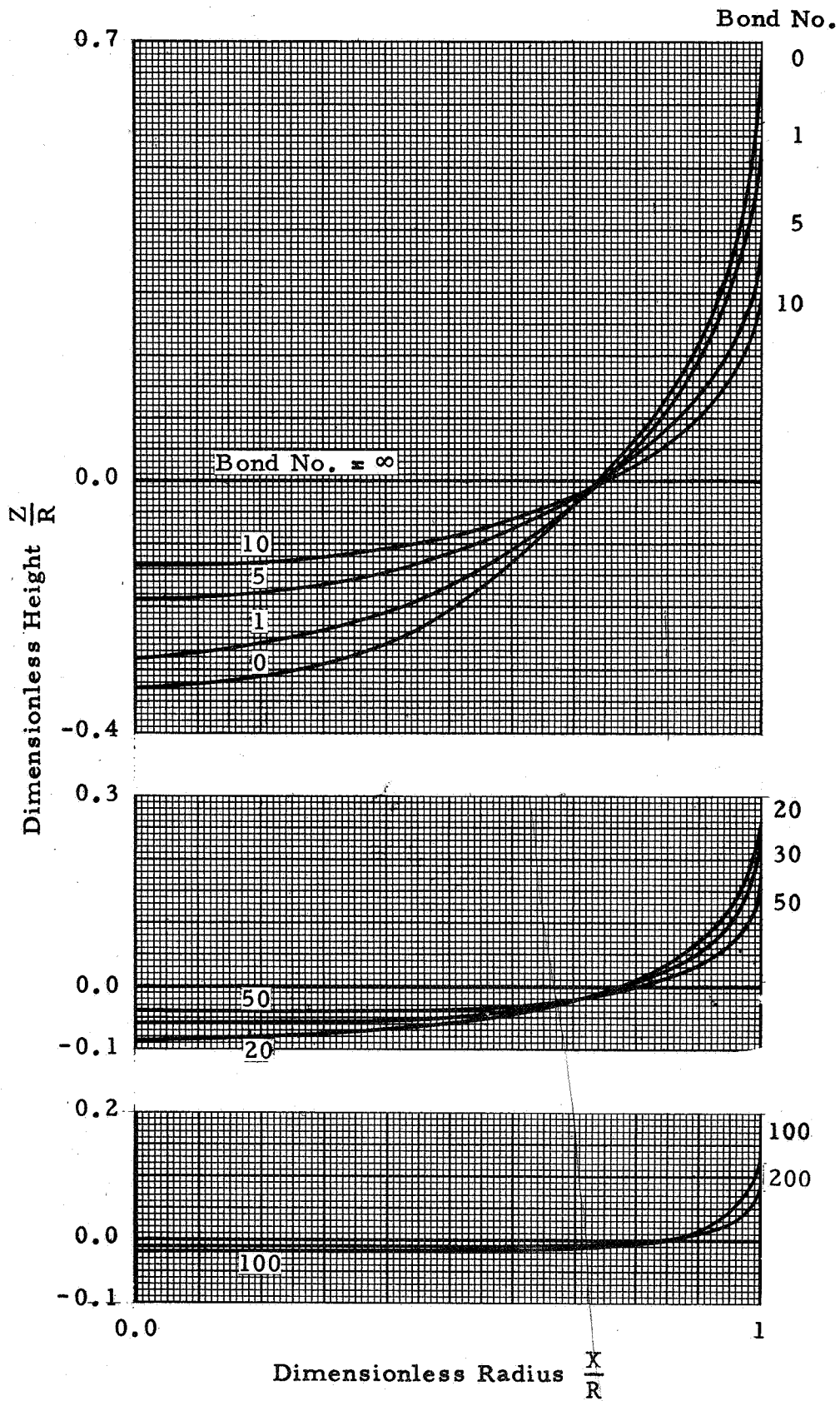


FIGURE 4. LOW GRAVITY ZERO CONTACT ANGLE INTERFACE SHAPES IN CYLINDRICAL CONTAINERS

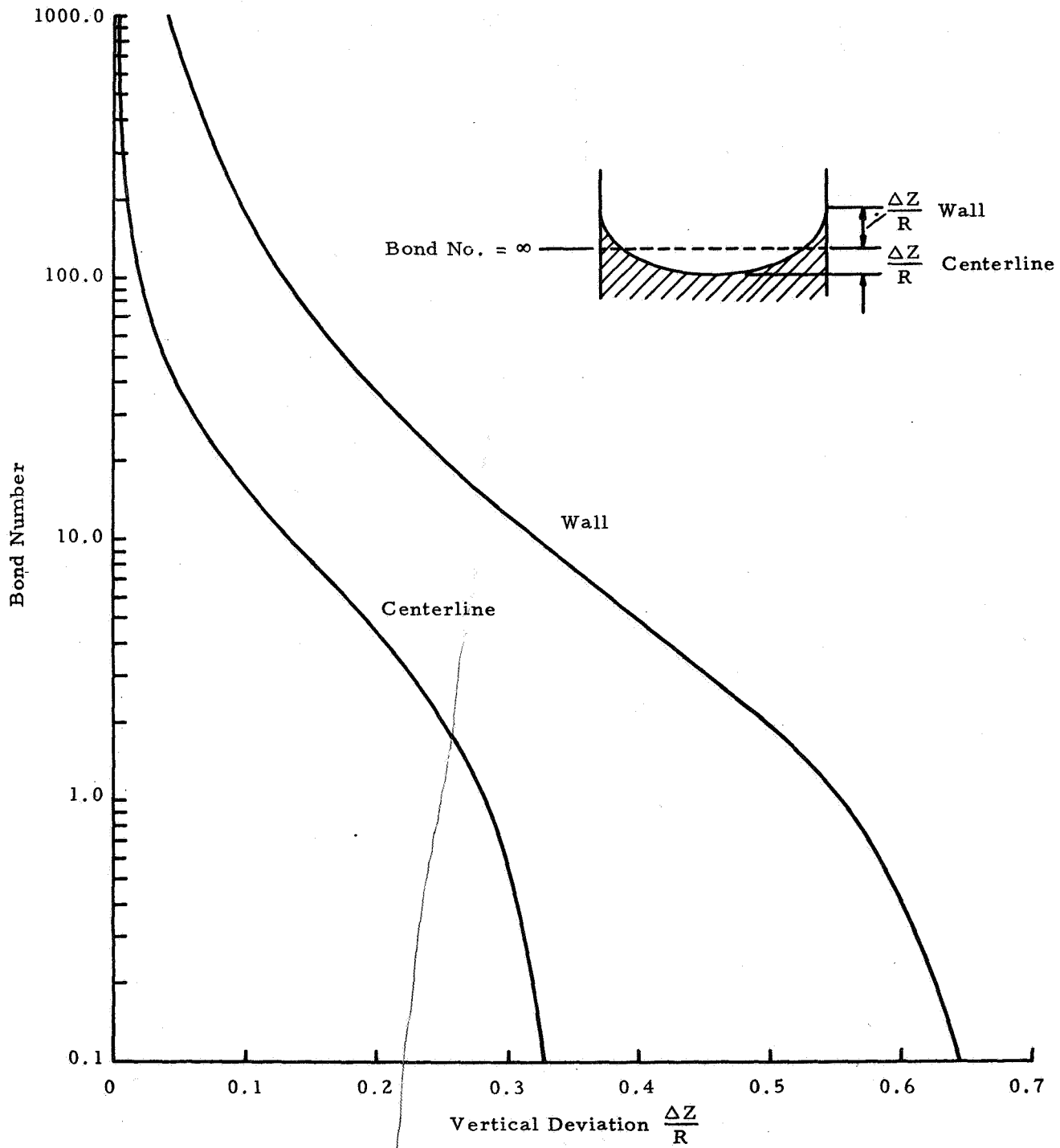


FIGURE 5. ZERO CONTACT ANGLE INTERFACE DEVIATION FROM THE INFINITE BOND NUMBER LEVEL IN A CYLINDER

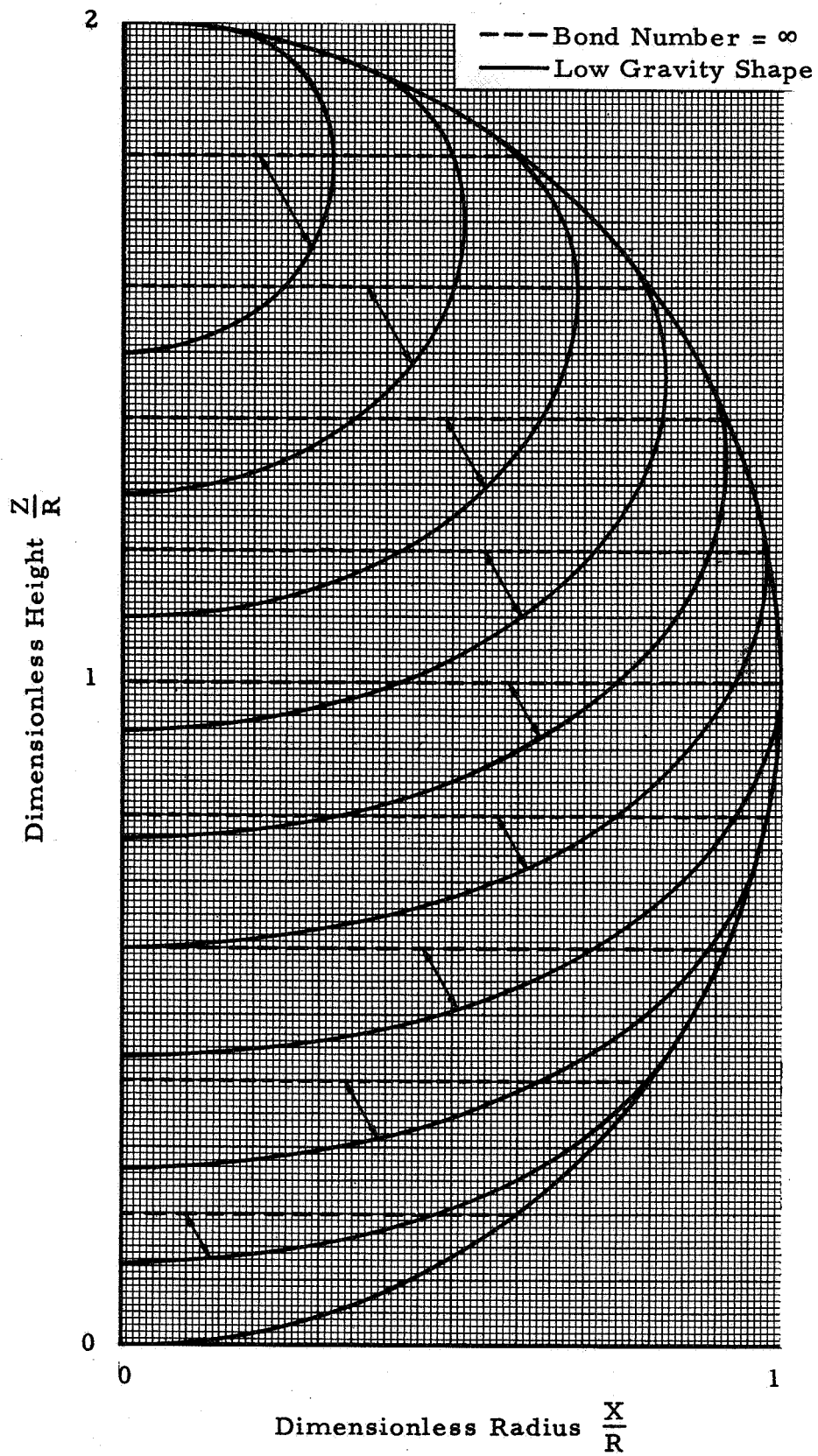


FIGURE 6. ZERO CONTACT ANGLE INTERFACE SHAPES IN SPHERICAL CONTAINERS FOR BOND NUMBER = 5

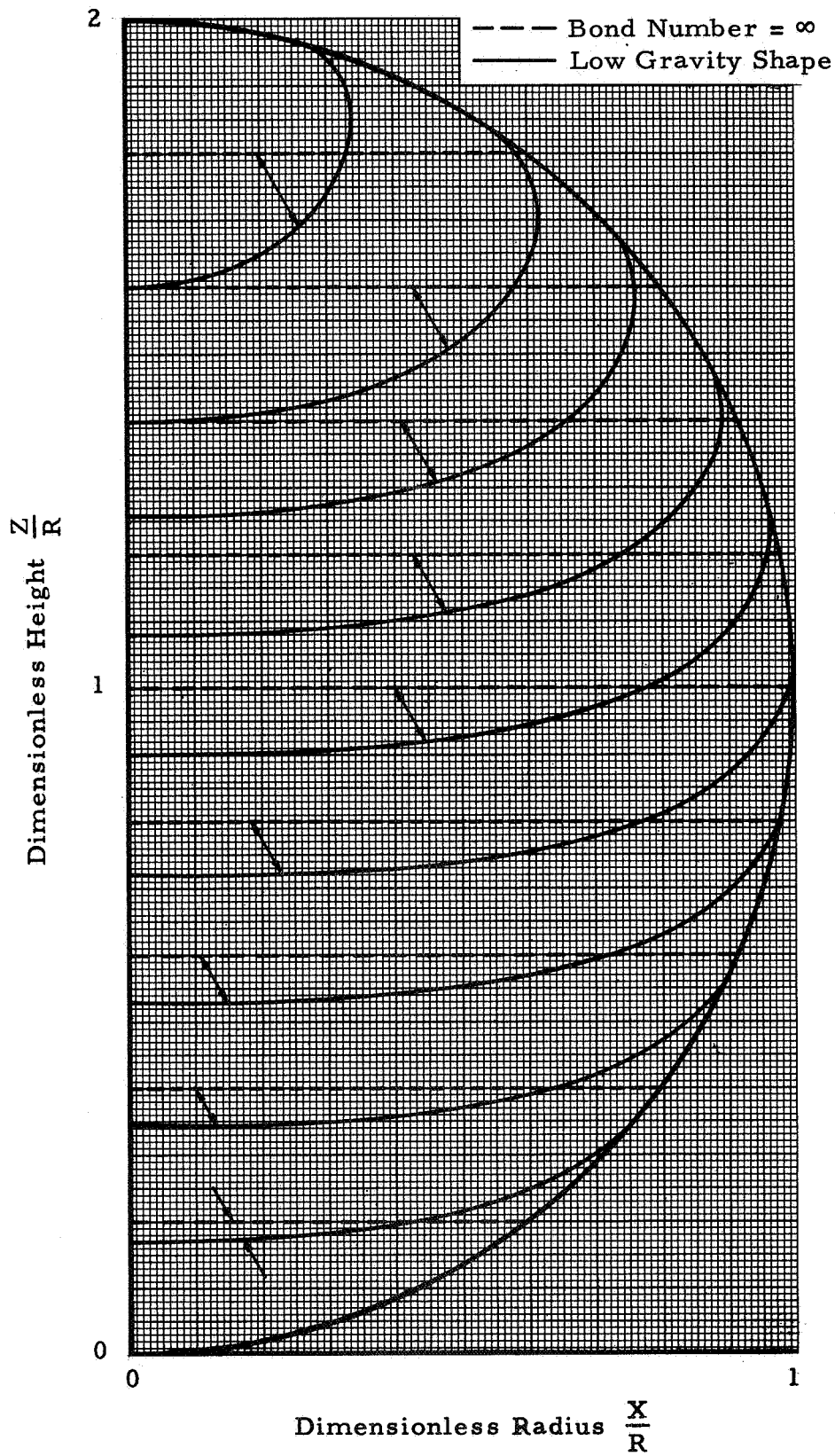


FIGURE 7. ZERO CONTACT ANGLE INTERFACE SHAPES IN SPHERICAL CONTAINERS FOR BOND NUMBER = 20

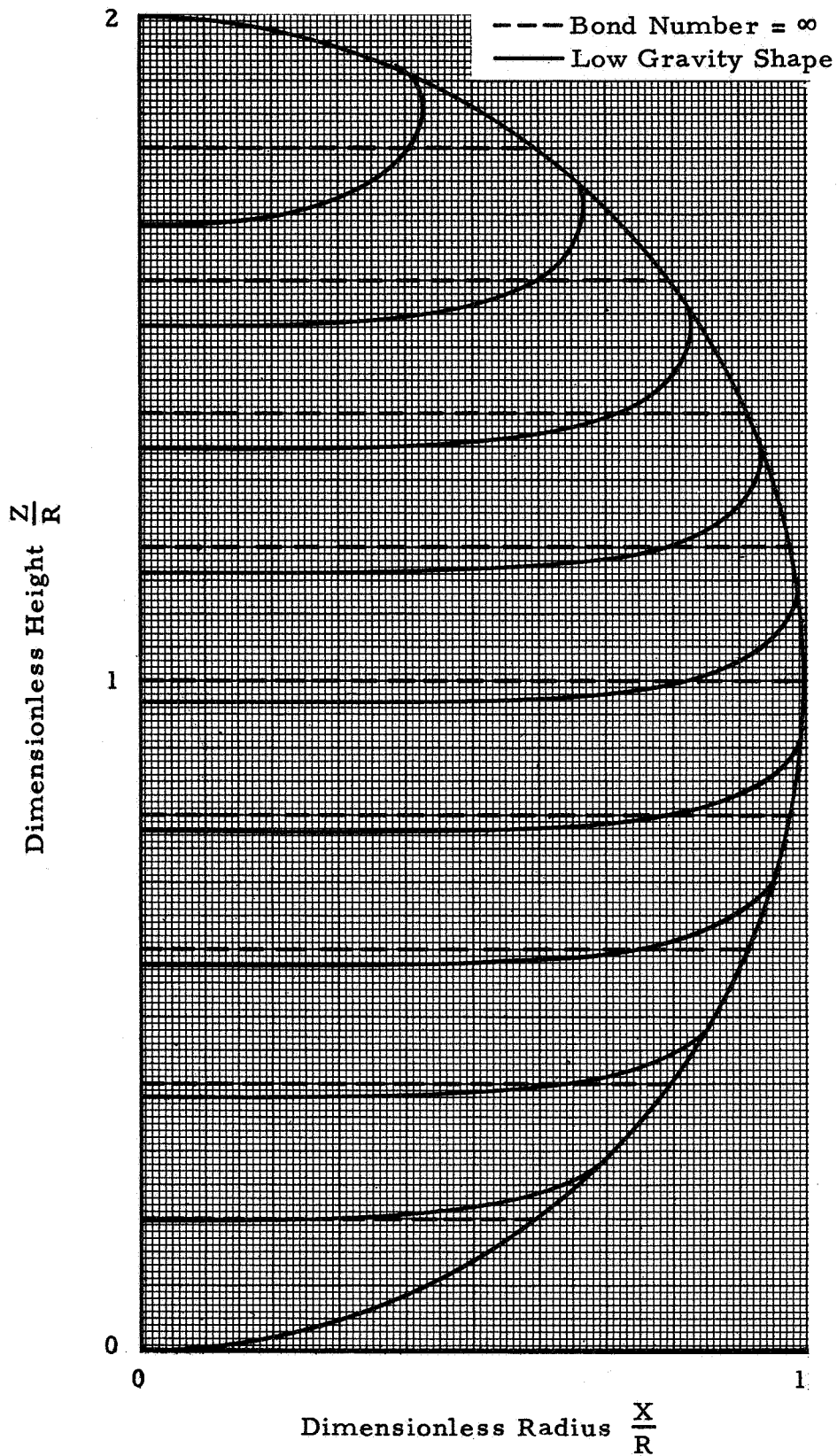


FIGURE 8. ZERO CONTACT ANGLE INTERFACE SHAPES IN SPHERICAL CONTAINERS FOR BOND NUMBER = 70

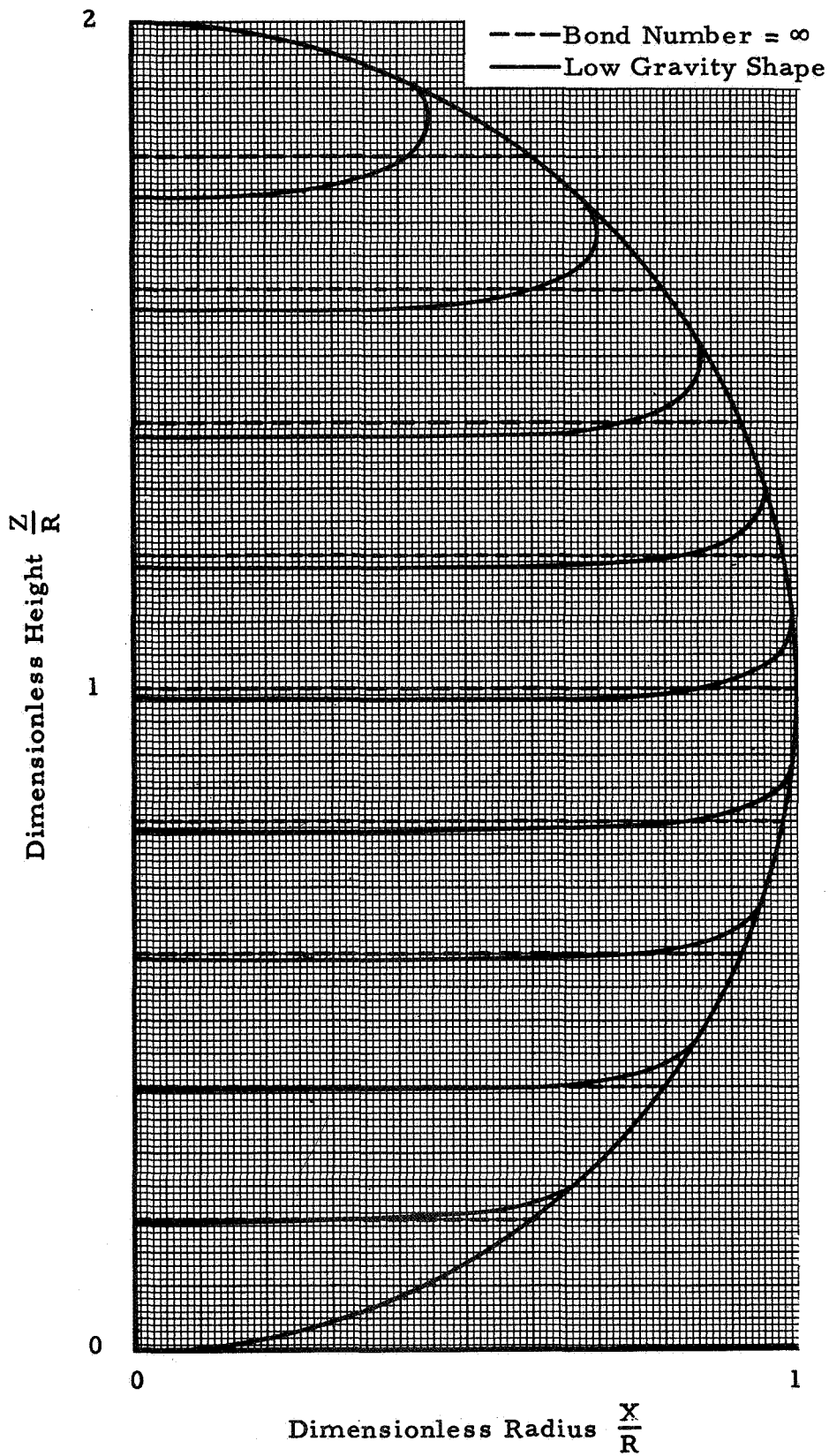


FIGURE 9. ZERO CONTACT ANGLE INTERFACE SHAPES IN SPHERICAL CONTAINERS FOR BOND NUMBER = 150

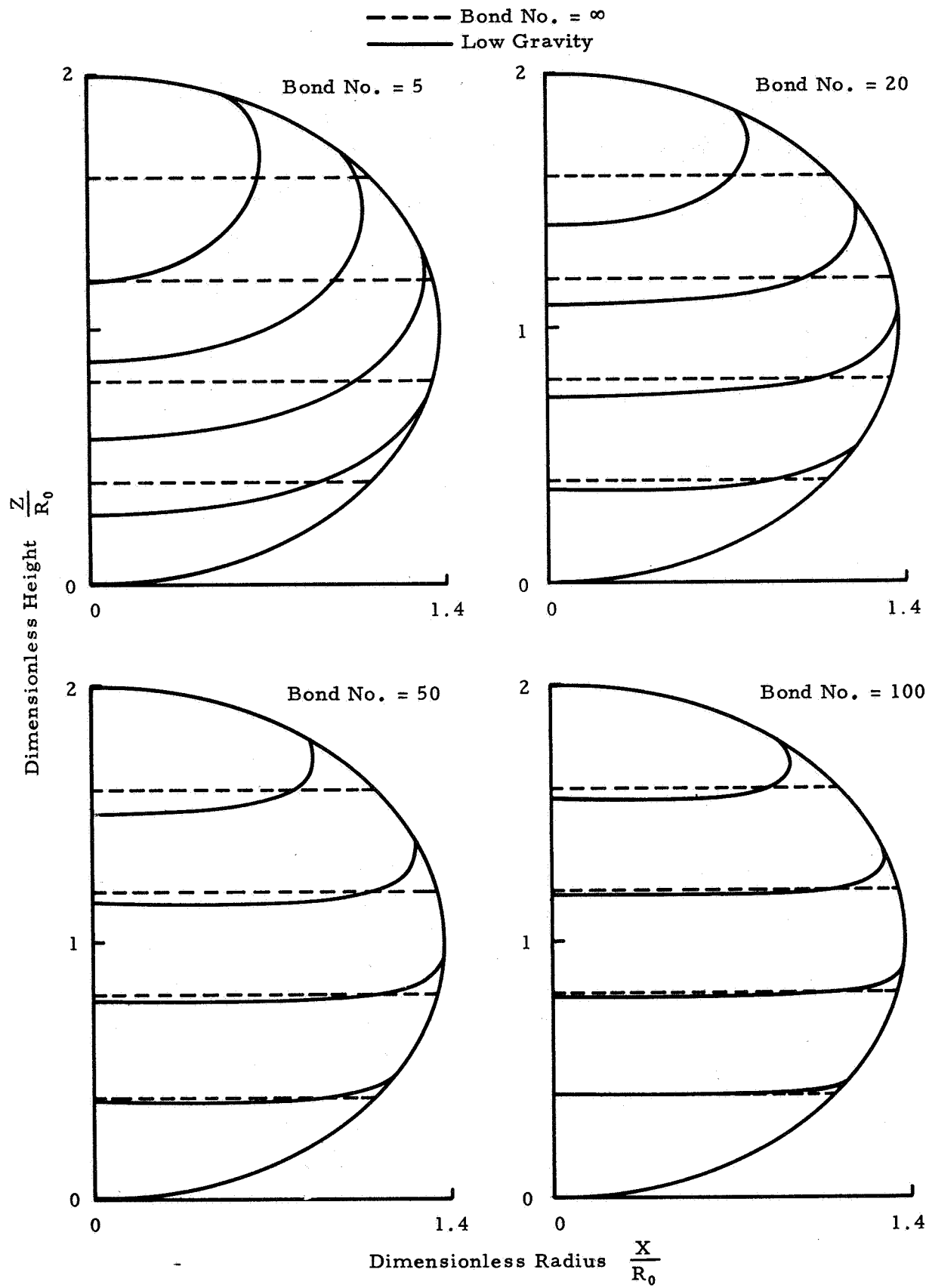


FIGURE 10. ZERO DEGREE CONTACT ANGLE INTERFACE SHAPES IN AN OBLATE SPHEROID

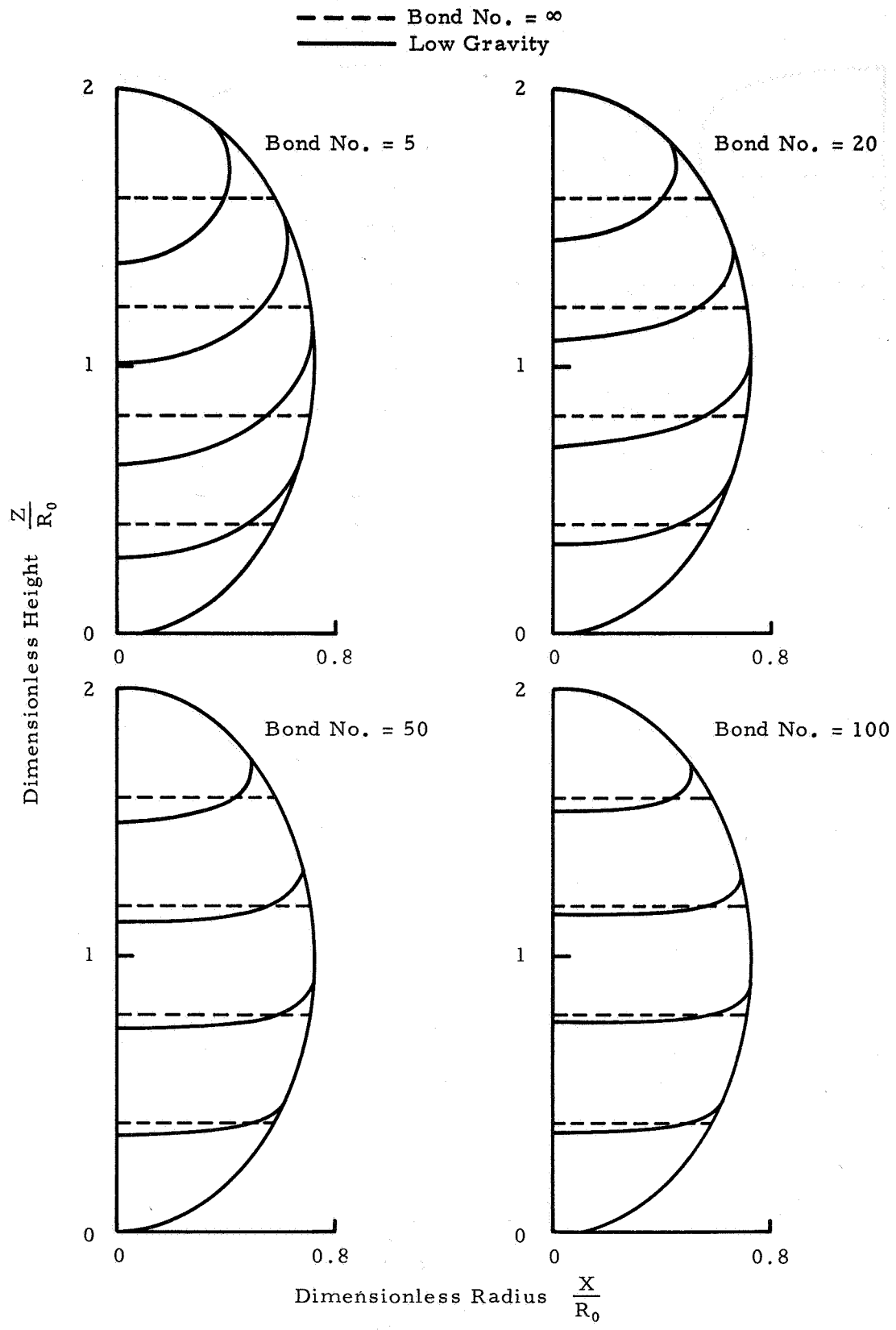


FIGURE 11. ZERO DEGREE CONTACT ANGLE INTERFACE SHAPES IN A PROLATE SPHEROID

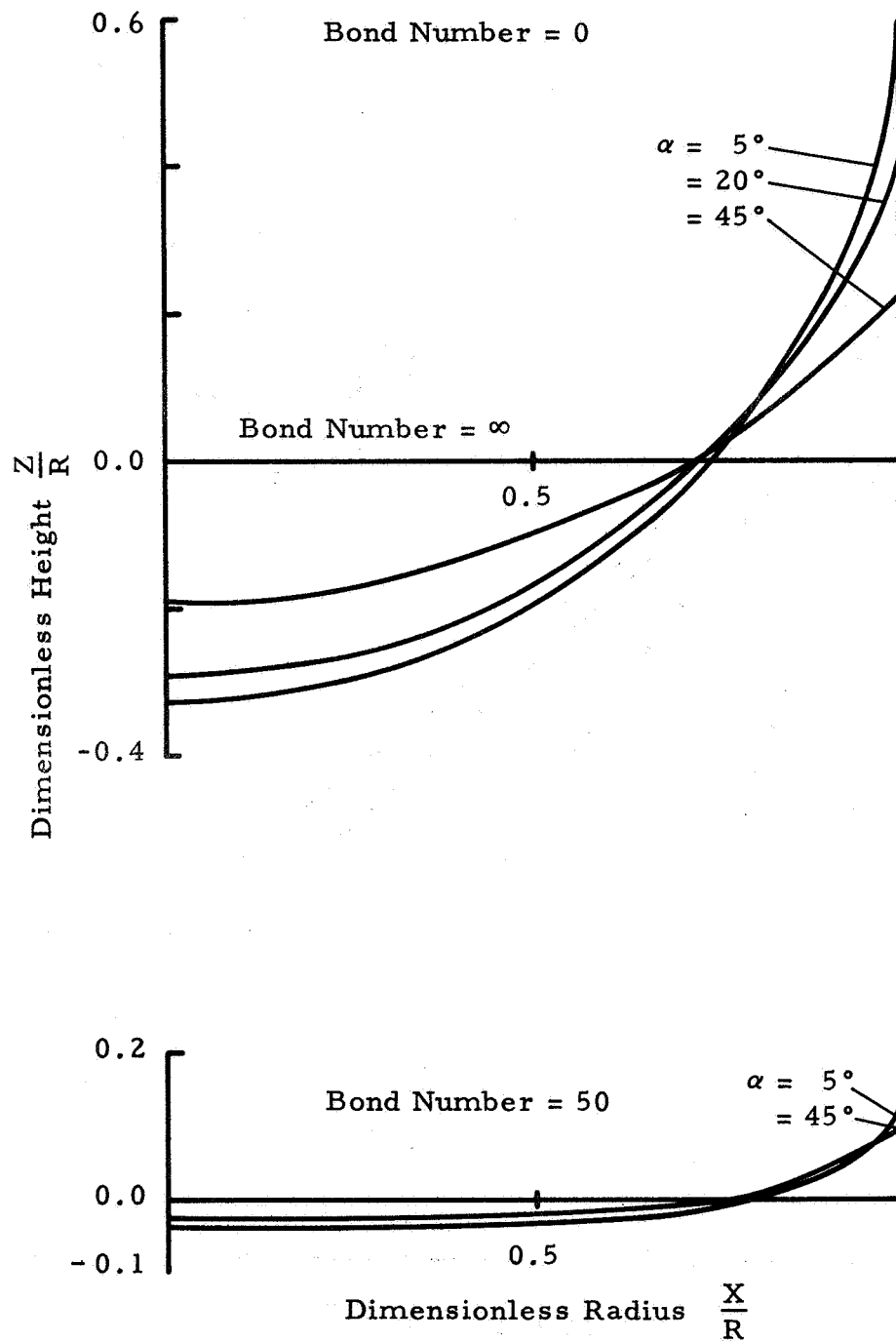


FIGURE 12. EFFECT OF CONTACT ANGLE ON SURFACE SHAPES IN A CYLINDER

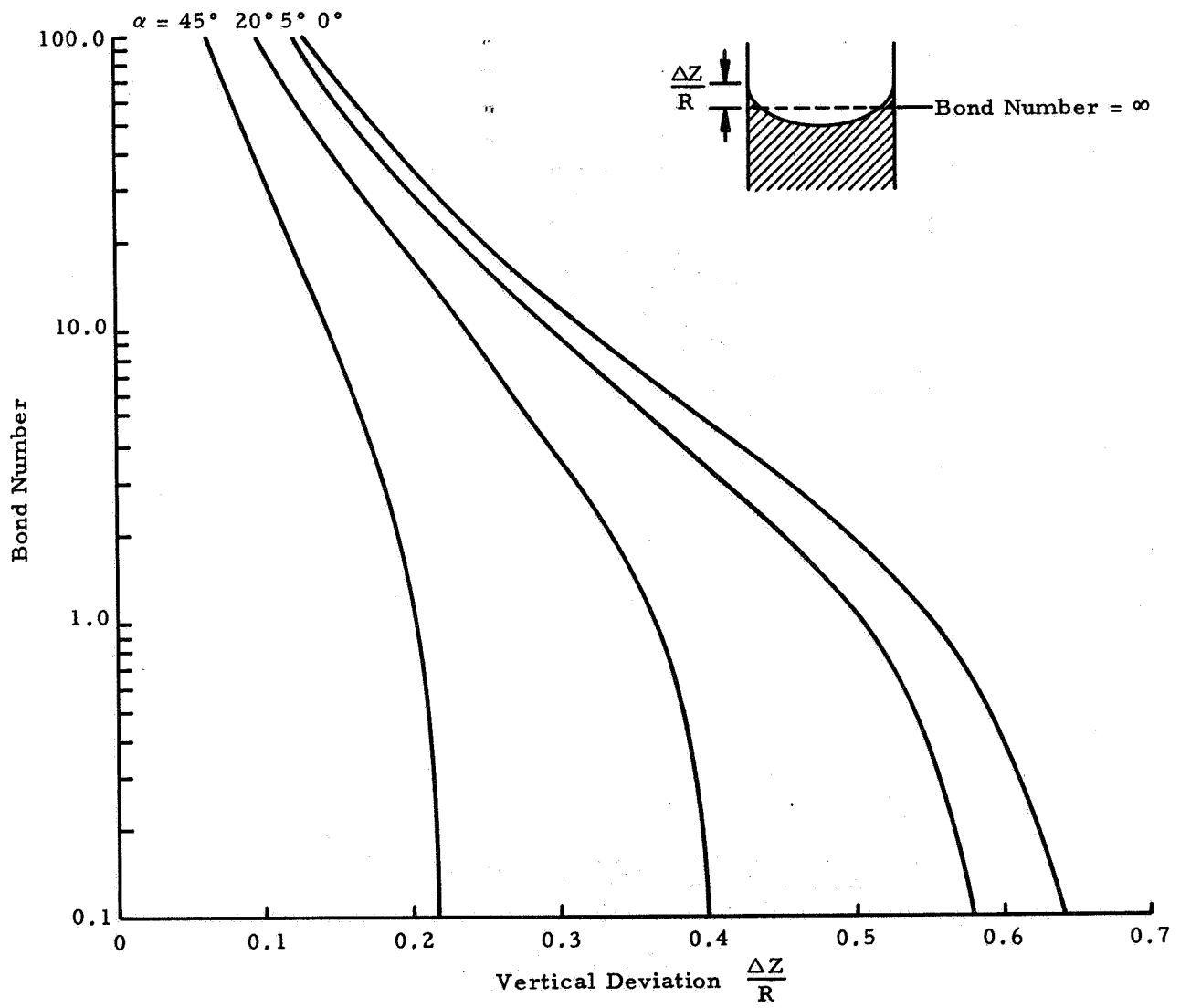


FIGURE 13. CONTACT ANGLE INFLUENCE ON SURFACE DEVIATION FROM THE INFINITE BOND NUMBER POSITION IN A CYLINDER

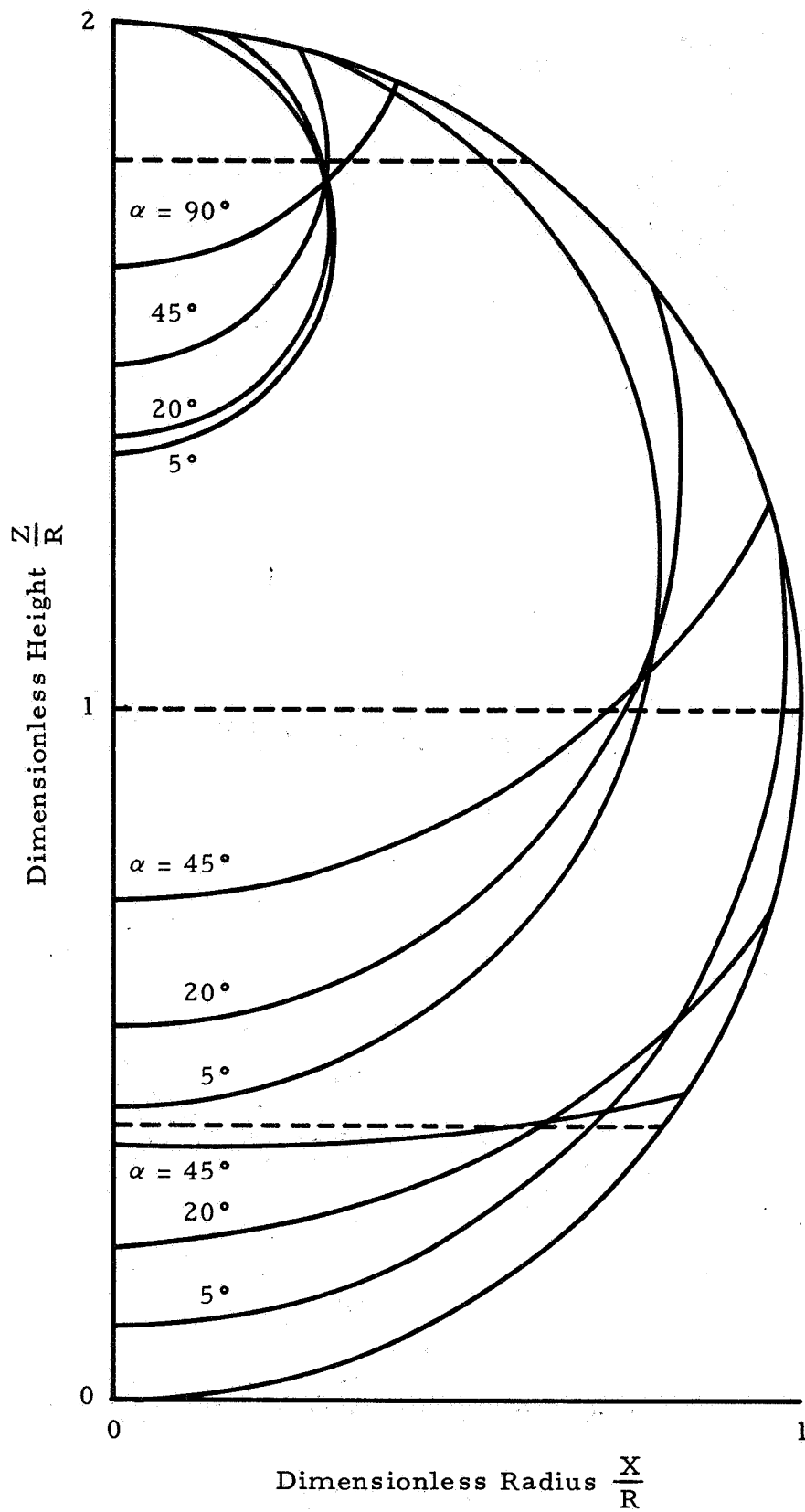


FIGURE 14. EFFECT OF CONTACT ANGLE ON SURFACE SHAPES IN A SPHERE AT BOND NUMBER = 0

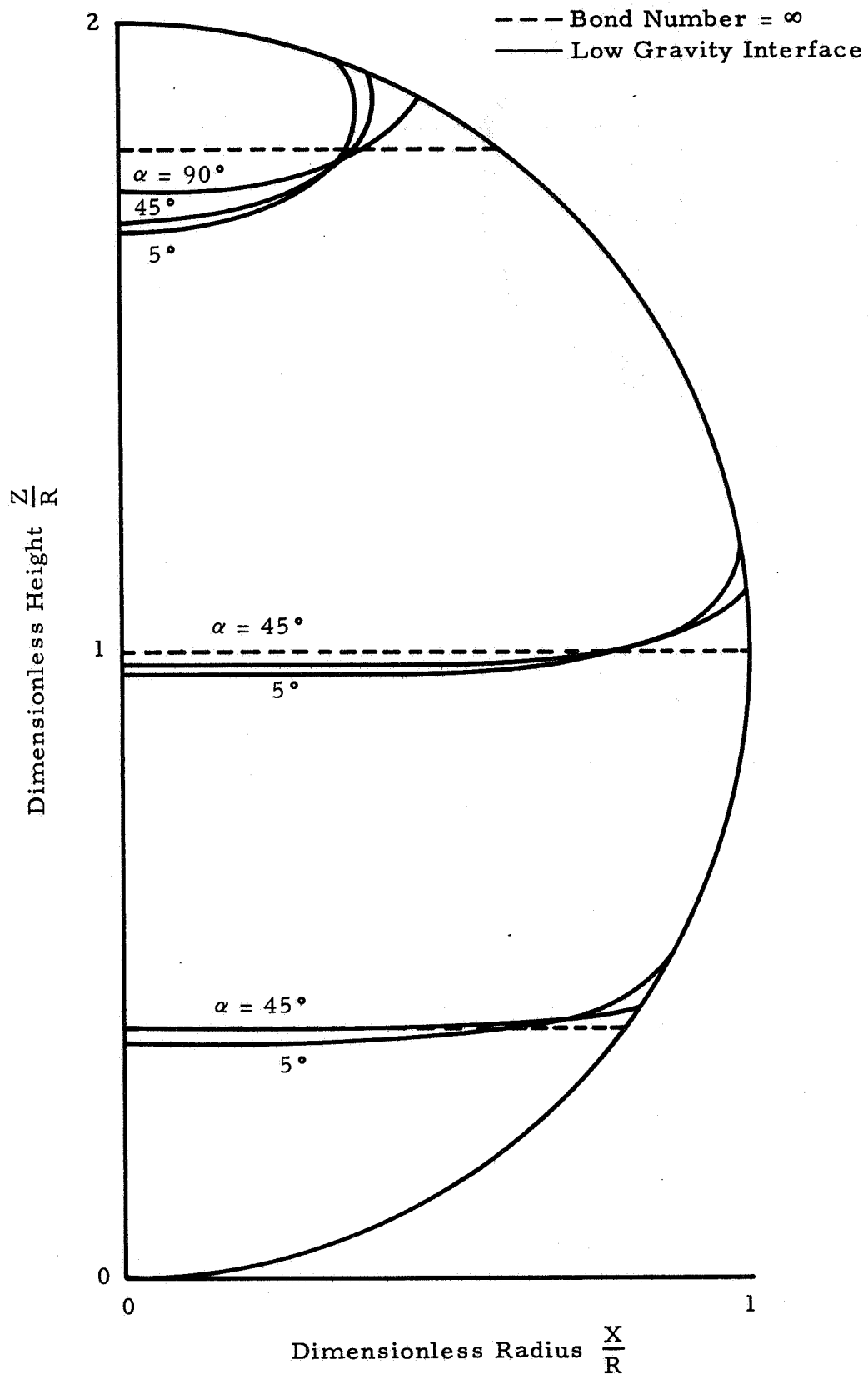


FIGURE 15. EFFECT OF CONTACT ANGLE ON SURFACE SHAPES IN A SPHERE AT BOND NUMBER = 50

VI. EXPERIMENTAL VERIFICATION

Experimental surface shapes for various Bond numbers and liquids in cylindrical containers were measured in normal gravity by personnel at Lockheed Missiles and Space Company, and are described in Reference 16. The Lockheed Company data are used herein to verify the theoretical solution presented in this report.

The test equipment and procedure used by Lockheed was relatively simple. The test containers were fabricated from Lucite blocks approximately 2 x 2 x 4 inches by drilling and polishing holes of various diameters in the blocks. The experimental procedure consisted simply of placing the test liquid in containers of various diameters, thereby varying Bond number, and photographing the meniscus shape.

The measured meniscus was corrected for distortion by calculating correction factors based on basic laws of reflection and refraction. The calculated correction factors were checked and verified by reading photographs of ball bearings with known dimensions. This procedure yielded accurate results except very near the cylinder walls where distortion was greatest. As mentioned in Reference 16, because of distortion problems, difficulties were encountered in determining exactly where the interfaces intersected the container walls, and accurate contact angle measurements were not possible.

Lockheed measured surface shapes for Bond numbers ranging from 8 to 53 using three test liquids: water, carbon tetrachloride, and methyl alcohol. Contact angles of 66, 18, and 17 degrees were specified for the water, carbon tetrachloride, and alcohol, respectively. However, the contact angles specified for carbon tetrachloride and alcohol are believed to be incorrect for the following reasons:

1. Lockheed investigators did not express confidence in the measured contact angles.

2. Contact angles of zero degrees are usually quoted in literature for carbon tetrachloride and methyl alcohol in contact with glass or Lucite. (References 17 and 18.)

3. The theoretical shapes calculated by Lockheed indicated that the actual contact angles were lower than the measured values.

The measured contact angle for water should be correct since the measurement accuracy for such large angles should be good.

Using contact angles of zero degrees for carbon tetrachloride and alcohol and 66 degrees for water, theoretical surface shapes were determined and are compared with the Lockheed experimental data in Figures 16 through 18. As illustrated in these figures, the theoretical profiles agree exceptionally well with the experimental data. In fact, if the actual contact angle is known, it is believed that the static equilibrium interface profiles can be computed with greater accuracy than they can be measured due to the distortion and reflection problems inherent in such experimental measurements.

Attempts have been made to obtain additional experimental data in actual low gravity environments provided by the Marshall Space Flight Center (MSFC) drop tower facility. Cylindrical and spherical containers six inches in diameter were utilized with petroleum ether, a zero contact angle liquid, as the test fluid. However, when a liquid-vapor system is subjected to a sudden decrease in acceleration, such as that encountered in drop tower testing, certain interface oscillations must occur before the equilibrium configuration is attained. Theoretical and experimental evaluations of such interface oscillations have been presented by Paynter, Fung, and Siegret, et al in References 19, 20, and 21, respectively.

The maximum test time available in the MSFC drop tower (4.3 seconds) was insufficient to permit the interface to attain complete equilibrium. Thus, at best, the surface profiles attained only a state of quasi-equilibrium and the data can not be used to accurately verify theoretical interface solutions. However, based on preliminary comparisons, it can be stated that the experimental profiles did appear to oscillate about the theoretical static equilibrium shapes. It is anticipated that this drop tower data will be published in a MSFC document in the near future.

— Theoretical Zero Contact Angle Surface
 ○ Experimental Data From Ref. 16

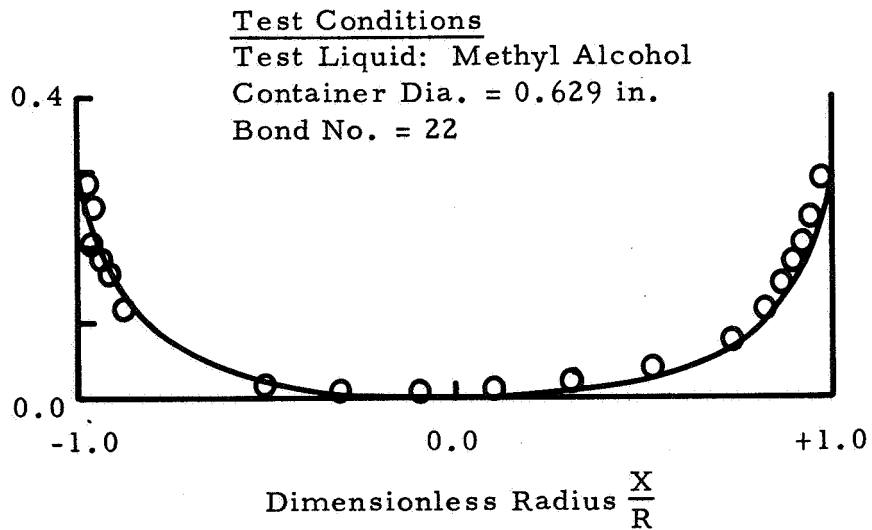
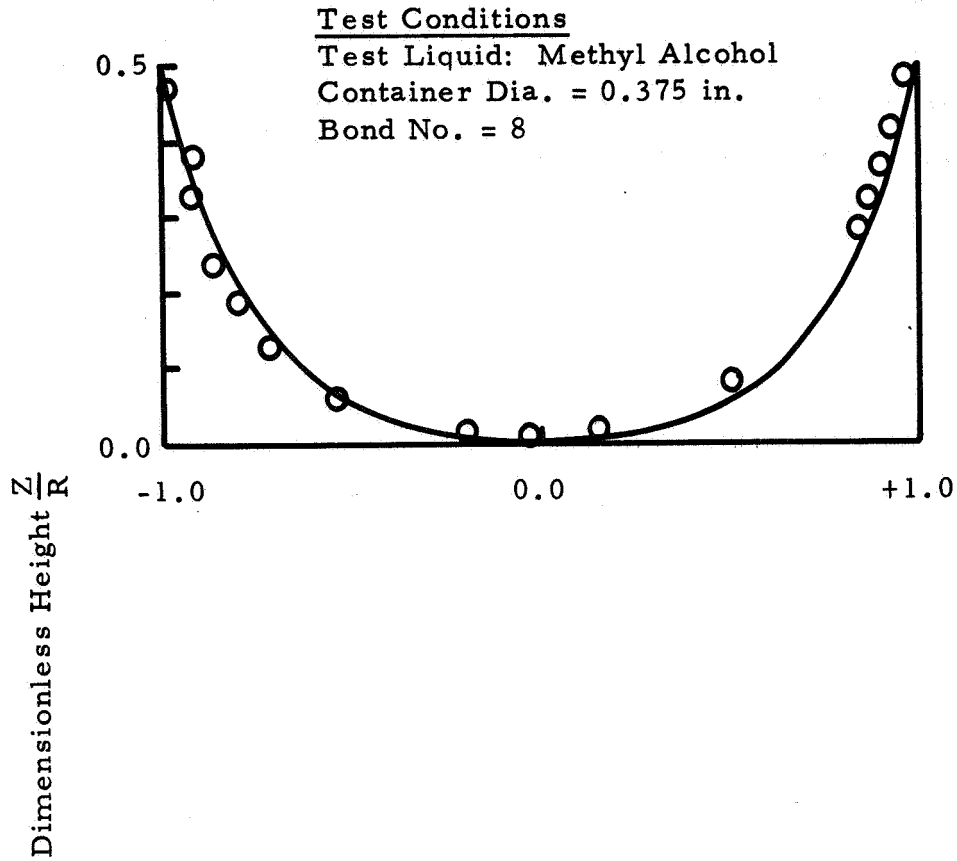
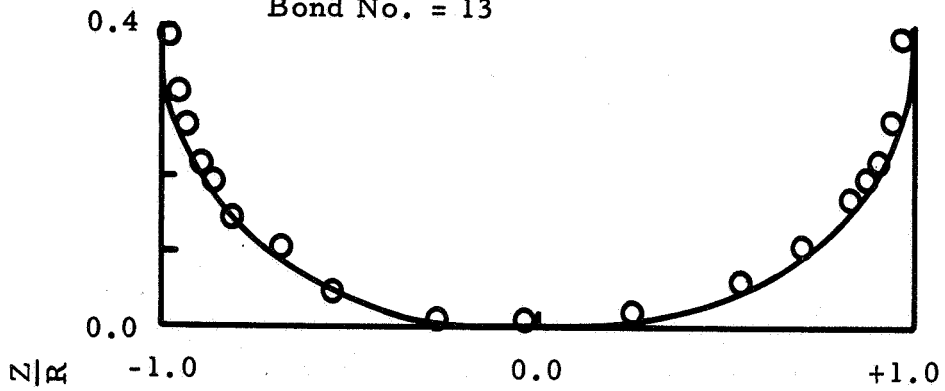


FIGURE 16. EXPERIMENTAL AND THEORETICAL INTERFACE SHAPES IN A CYLINDER

— Theoretical Zero Contact Angle Surface
 ○ Experimental Data From Ref. 16

Test Conditions

Test Liquid: Carbon Tetrachloride
 Container Dia. = 0.375 in.
 Bond No. = 13



Test Conditions

Test Liquid: Carbon Tetrachloride
 Container Dia. = 0.75 in.
 Bond No. = 53

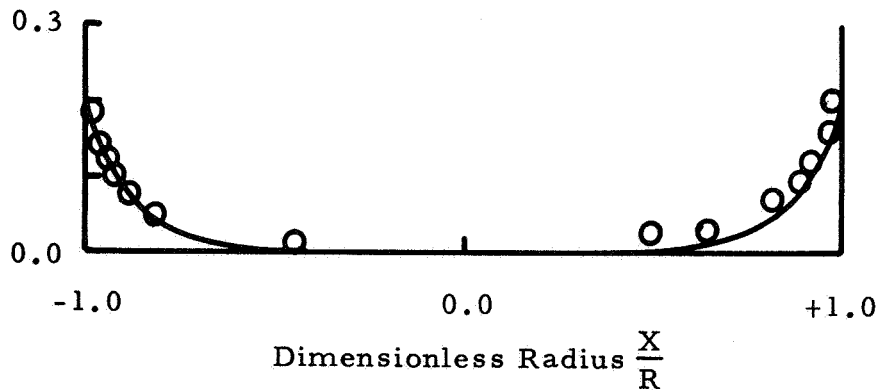


FIGURE 17. EXPERIMENTAL AND THEORETICAL INTERFACE SHAPES IN A CYLINDER

— Theoretical Surface For Contact Angle = 66°
○ Experimental Data From Ref. 16

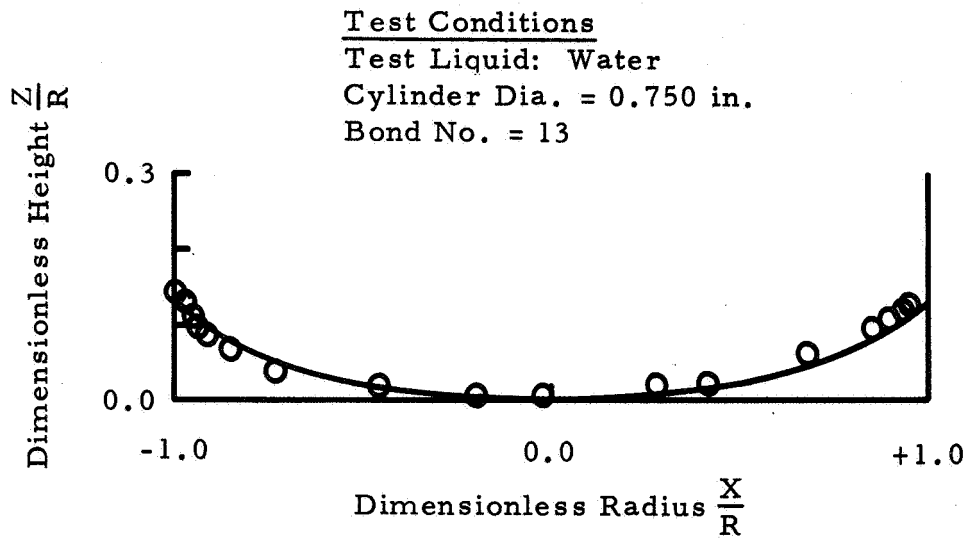


FIGURE 18. EXPERIMENTAL AND THEORETICAL INTERFACE SHAPES IN A CYLINDER

VII. CONCLUSIONS

Based on the theoretical and experimental data acquired by these and other investigators, the following conclusions are made.

1. Use of a polar coordinate system in developing the basic differential equation for liquid-vapor interface profiles eliminates convergence difficulties encountered in the solution of previously developed differential equations.

2. The polar coordinate system enabled the incorporation of a Bond number based on a container dimension into the basic differential equation as opposed to a Bond number based on interface radius of curvature.

3. Using the Runge-Kutta numerical technique, the interface equation developed herein can be readily solved by a computer. The method imposes no significant limitations on contact angle or Bond number.

4. The effect of contact angle on surface shapes decreases with increasing Bond number and becomes negligible as the zero degree contact angle liquid surface approaches flatness.

5. The theoretical equilibrium interface profiles, determined using the methods presented herein, correlate well with experimentally measured surface profiles.

6. Due to the distortion and reflection problems inherent in measuring actual surface profiles and contact angles, it appears that the profiles can in most cases be theoretically calculated with greater accuracy than the surfaces can be measured.

[The page contains extremely faint and illegible text, likely bleed-through from the reverse side of the paper. The text is too light to transcribe accurately.]

APPENDIX A

LIQUID-VAPOR-SOLID INTERFACES

That the shape of a droplet can be significantly affected by the presence of a solid is a well known observation. The degree to which the liquid-vapor interface shape is influenced is dependent on whether the cohesive* or adhesive* forces dominate, that is, the "wettability". The term "wettability", sometimes called "spreadability" is easily illustrated by noting a common, everyday occurrence; the effects of waxed and unwaxed surfaces on liquid droplet behavior. Droplets of water on the waxed surface will form "beads", while water on the unwaxed surface rapidly spreads or wets the surface. Whenever the degree of attraction between the liquid and solid is discussed (wettability) the term usually invoked is "contact angle".

Contact angle, as described in Figure 1A, is the angle (measured in the liquid) between the solid-liquid and the liquid-vapor interfaces. If a contact angle less than 90 degrees exists, the surface is said to be wetted; a contact angle greater than 90 degrees denotes a "non-wetting" of the surface. Many liquid-solid surfaces demonstrate total wetting, i. e., contact angles of zero degrees; but it is impossible to have a perfectly non-wetting liquid-solid surface, i. e., a contact angle equal to 180 degrees. The only liquid approaching complete non-wettability is mercury, which has a contact angle of about 125 degrees on glass surfaces.

* These terms are defined in this study under "Basics of Liquid-Vapor-Solid Systems".

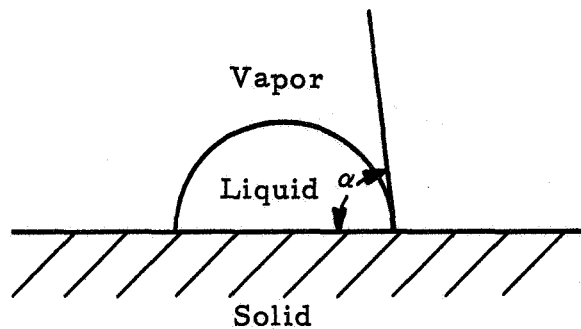


FIGURE 1A. CONTACT ANGLE MEASUREMENT

Over 150 years ago, Thomas Young proposed treating the contact angle of a liquid as the result of the mechanical equilibrium of three surface tensions acting on the line of contact between a liquid-gas interface and a solid surface. These surface tensions are usually termed the solid-vapor (σ_{sv}), liquid-solid (σ_{ls}), and liquid-vapor (σ_{lv}) surface tensions and are assumed to act in a direction parallel to each of their respective interfaces at the line of contact (see Figure 2A). This line of contact can be displaced to increase the solid-gas interface at the expense of the solid-liquid interface. If the solid-liquid surfaces exerted no force upon the line of contact, then obviously no equilibrium position would be possible since a force, $\sigma_{lv} \cos \theta$, parallel to the solid surface acts on this line.

There must, therefore, be forces of the same nature as surface tensions that act through the line of contact, P, and are associated with the solid-vapor and solid-liquid interfaces. Young (Ref. 22) proposed that contact angle be related to the surface tensions of the three surfaces by the relation

$$\sigma_{lv} \cos \alpha = \sigma_{sv} - \sigma_{sl} \quad (1A)$$

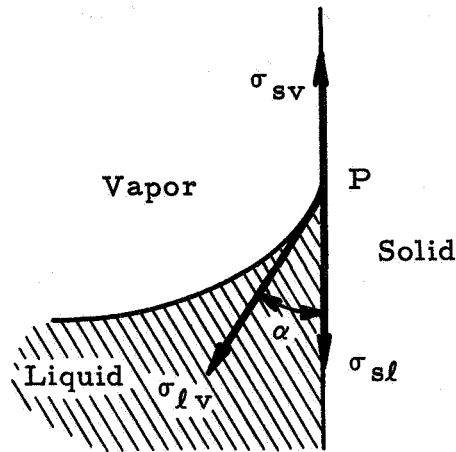


FIGURE 2A. SURFACE TENSIONS AT A LIQUID-VAPOR-SOLID INTERFACE

Since the solid-vapor and solid-liquid surface tensions are not well understood and are difficult if not impossible quantities to measure experimentally, Young's equation is an extremely useful tool in that it expresses the effects of these surface tensions in terms of measurable quantities, that is, contact angle and liquid-vapor surface tension. However, the relation is deceptively simple and has been the source of many arguments. Bikerman (Ref. 23) has criticized the equation on the grounds that the equilibrium conditions are discussed only with respect to forces parallel to the surface, and that no account is taken of the component $\sigma_{lv} \sin \alpha$ normal to the solid surface.

A clear statement of the problem and a thermodynamic justification of Young's relation was given by Johnson (Ref. 24). Also, Lester (Ref. 25) has recently given a sophisticated treatment of the equation and showed that it is correct so long as the solid is not easily deformable.

In addition, the surface condition of a solid can significantly affect the contact angle of a liquid on the solid. One such effect, which was analyzed by Wenzel (Ref. 26), is surface roughness. It seems that liquid on a rough surface will exhibit lower contact angles than on a smooth one, because the surface irregularities provide many capillary

paths for the liquid and thereby cause the liquid to spread. Wenzel suggested a modified form of equation (1A)

$$\sigma_{lv} \cos \alpha = r(\sigma_{sv} - \sigma_{sl}) \quad (2A)$$

where α is the average apparent contact angle and r is the ratio of true to apparent area of the solid.

A second influence on contact angle is the presence of molecules adsorbed at the solid interface. This influence was observed by Langmuir (Ref. 27) when he measured a contact angle hysteresis effect whenever the line of contact between the liquid and solid was in motion, that is, the measured contact angle depended on whether the boundary was advancing or receding. Langmuir attributed this variation in contact angle to a monomolecular layer that was adsorbed when liquid advanced over the surface and thereby decreased the contact angle when the liquid receded.

In conclusion, the use of Young's equation and the concept of contact angle appears to be valid if the restrictions involved are properly understood. If further information on liquid-solid-vapor interfaces is desired, Reference 28 contains a comprehensive summary of recent works on the subject.

APPENDIX B

BOUNDARY CONDITIONS DEPENDENT ON CONTAINER SHAPE

The expressions for boundary conditions that are dependent on container shape are developed in this Appendix. As noted previously, the liquid-vapor interface shapes are symmetrical about the vertical axis, and therefore, the relations for container boundary and contact angle can be formulated based on a vertical cross-section of the container.

A. Prolate and Oblate Spheroids

Referring to Figure 1B, the equations for container boundary (Y_B) contact angle (α), and empty fraction (β) are derived as follows:

1. Container Boundary - In this study, the equation for a vertical cross-section of both a prolate and oblate spheroid (an ellipse) is non-dimensionalized with respect to the vertical semi-axis of the ellipse, i.e., the Z/R_0 intercepts are always (0, -2). Therefore, the boundary for an ellipse is defined by the single relation

$$Y_B = \frac{2 b^2 \cos \theta}{\sin^2 \theta + b^2 \cos^2 \theta} \quad (1B)$$

where "b" is always the horizontal dimension. Therefore,

$$\begin{aligned} b < 1 & \text{ Prolate Spheroid} \\ b > 1 & \text{ Oblate Spheroid} \end{aligned}$$

2. Contact Angle - As proven in Reference 29, the acute angle, ψ , between the tangent to the boundary, $Y_B = y(\theta)$, at point "P" and the line \overline{OP} is defined by the relation

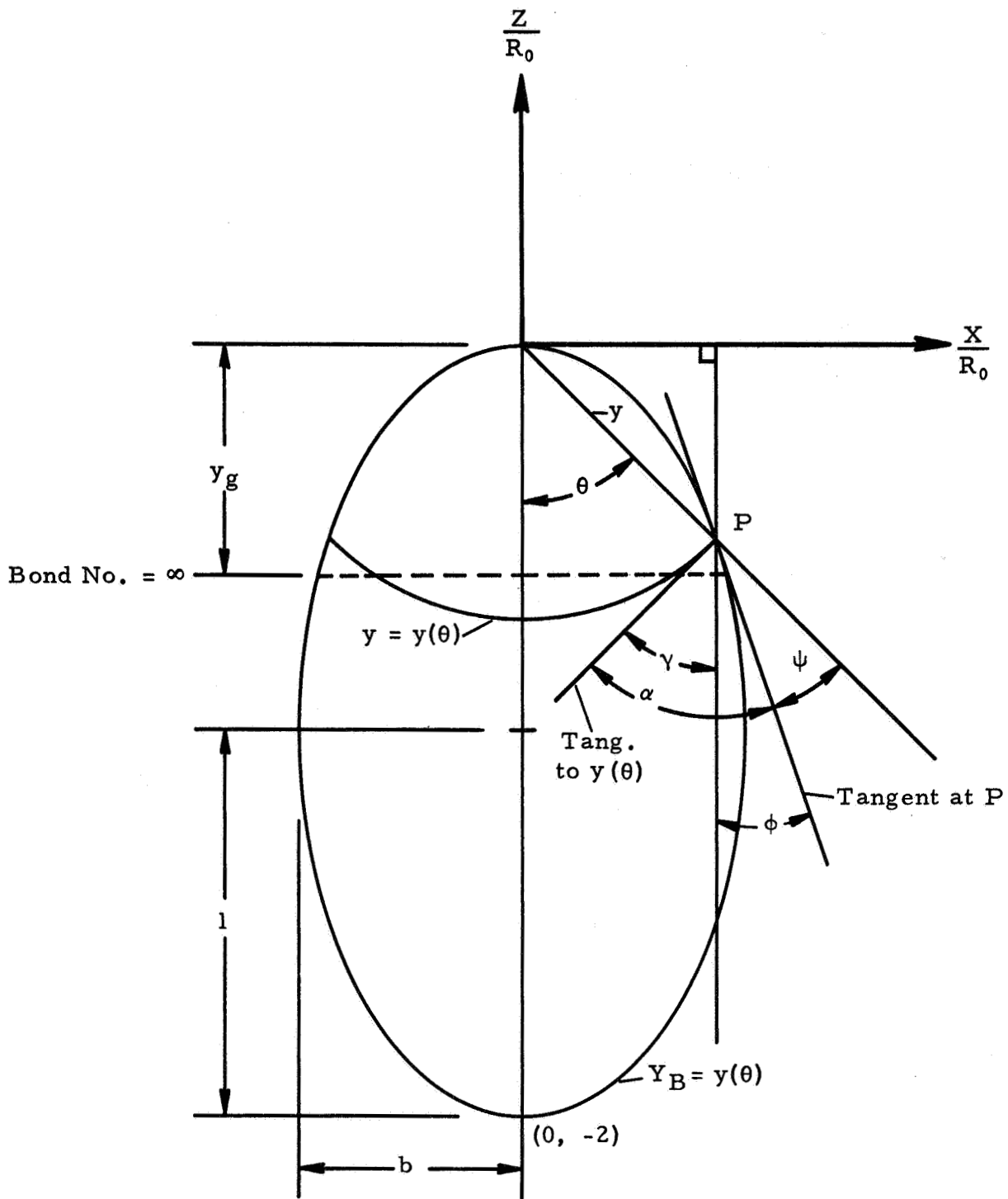


FIGURE 1B. GEOMETRY FOR PROLATE AND OBLATE SPHEROID BOUNDARY CONDITIONS

$$\tan \psi = - \frac{y(\theta)}{y'(\theta)} \quad (2B)$$

Since

$$y(\theta) = \frac{2 b^2 \cos \theta}{\sin^2 \theta + b^2 \cos^2 \theta}$$

Performing the operation indicated in equation (2B) yields

$$\psi = \arctan \left[\frac{\cos \theta (\sin^2 \theta + b^2 \cos^2 \theta)}{\sin^3 \theta - b^2 \cos^2 \theta \sin \theta + 2 \sin \theta \cos^2 \theta} \right] \quad (3B)$$

Also, note that since $X = R_o y \sin \theta$ and $Z = - R_o y \cos \theta$ then the angle, γ , measured from the vertical \overline{MP} and the tangent to $y(\theta)$ at "P" can be specified as follows

$$\gamma = \arctan \left(\frac{dX}{dZ} \right) \text{ at point P}$$

$$\gamma = \arctan \left(\frac{y' \sin \theta + y \cos \theta}{y \sin \theta - y' \cos \theta} \right) \quad (4B)$$

From the geometry of Figure 1B, it is apparent that the contact angle α is

$$\alpha = \gamma + \phi = \gamma + \theta - \psi \quad (5B)$$

Substituting in equation (5B) from relations (3B) and (4B) the final equation for contact angle is

$$\alpha = \arctan \left(\frac{y' \sin \theta + y \cos \theta}{y \sin \theta - y' \cos \theta} \right) + \theta - \arctan \left[\frac{\cos \theta (\sin^2 \theta + b^2 \cos^2 \theta)}{\sin^3 \theta - b^2 \cos^2 \theta \sin \theta + 2 \sin \theta \cos^2 \theta} \right] \quad (6B)$$

3. Empty Fraction - Since the equation for an ellipse with the origin at the top of the ellipse is

$$\frac{X^2}{b^2} + (Z + 1)^2 = 1$$

Then it is easily shown that for the total container volume (V_t) and vapor volume (V_v), the relations are

$$V_t = 2\pi \int_{-1}^0 X^2 dZ = \int_{-1}^0 b^2 [1 - (Z + 1)^2] dZ$$

$$V_t = \frac{4}{3} \pi b^2 \quad (7B)$$

and

$$V_v = \pi \int_{y_g}^0 b^2 [1 - (Z + 1)^2] dZ$$

$$V_v = \pi b^2 \left(y_g^2 - \frac{y_g^3}{3} \right) \quad (8B)$$

and empty fraction, β , is simply

$$\beta = \frac{V_v}{V_t} = \frac{3}{4} y_g^2 \left(1 - \frac{y_g}{3} \right) \quad (9B)$$

B. Spheres

It is a very simple matter to develop relations for the boundary conditions in a spherical container by setting the semimajor and semi-minor axes equal, i. e., set $b = 1$, in the equations for the spheroidal containers to make the relations applicable to a spherical cross section (circle). On inserting $b = 1$ in relations (1B), (6B), and (9B),

1. Container Boundary

$$Y_B = 2 \cos \theta \quad (10B)$$

2. Contact Angle

$$\alpha = 2\theta + \frac{180}{\pi} \arctan \left(\frac{y' \sin \theta + y \cos \theta}{y \sin \theta - y' \cos \theta} \right) - 90^\circ \quad (11B)$$

3. Empty Fraction

Since the equation for empty fraction in the spheroids is independent of "b", relation (9B) need not be changed for application to spherical containers.

C. Cylinders

The cylinder is the most simple geometrical configuration to analyze from the standpoint of interface shape since the container boundary is independent of the vertical coordinate "Z". Therefore, using Figure 2B to illustrate the geometry involved, it is easy to show that the boundary conditions for a cylinder are as follows:

1. Container Boundary - The vertical cross section of a cylindrical container that is symmetric about the vertical axis and of infinite height is prescribed by

$$|Y_B| = 1 \quad (12B)$$

2. Contact Angle - Contact angle is the slope of a tangent to the liquid-vapor interface/container boundary or

$$\alpha = \arctan \left(\frac{dX}{dZ} \right) \text{ at point P}$$

and,

$$\alpha = \arctan \left(\frac{y' \sin \theta + y \cos \theta}{y \sin \theta - y' \cos \theta} \right) \quad (13B)$$

3. Original Liquid Height - Since the interface shape in a cylinder of at least one container radius in depth is independent of the empty fraction, a calculation of β is not necessary to specify the interface in a cylinder. However, in order to designate the high gravity liquid level corresponding to the low gravity interface, it is necessary to compute the liquid volume participating in the interface deformation. The equation employed is

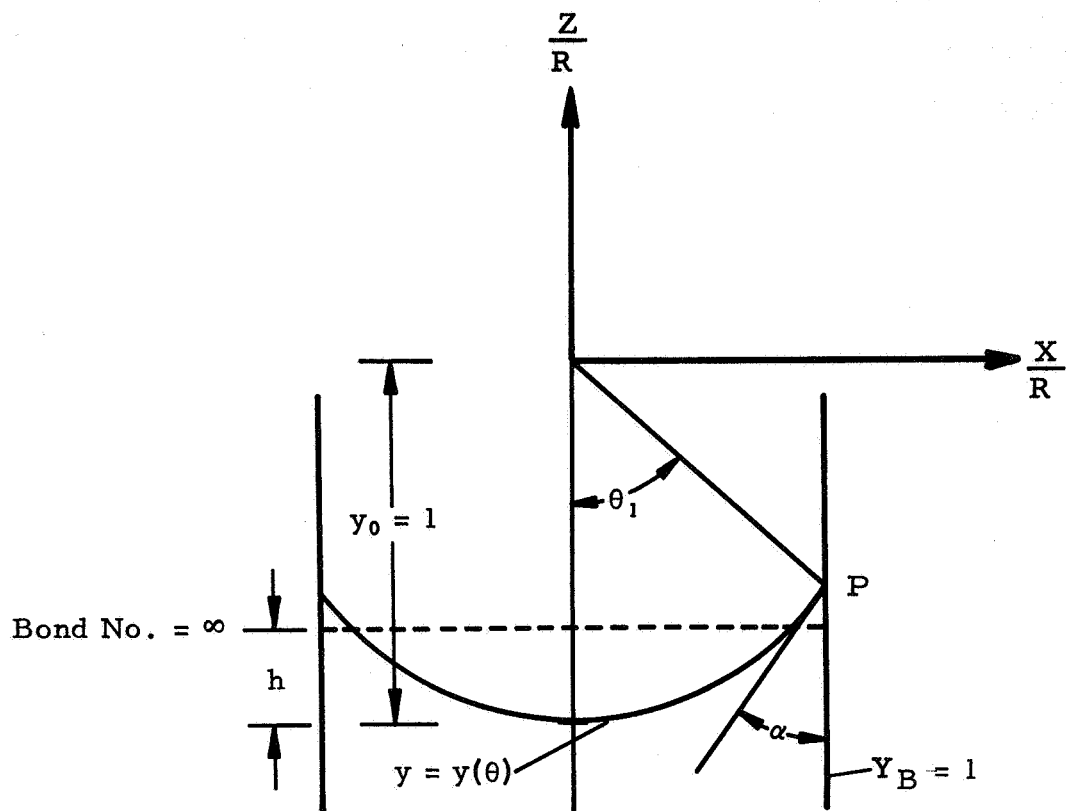


FIGURE 2B. GEOMETRY FOR BOUNDARY CONDITIONS IN A CYLINDER

$$d(V_{\ell}) = \pi \left[1 - \left(\frac{X}{R} \right)^2 \right] dZ$$

$$V_{\ell} = \int_0^{\theta_1} \pi (1 - y^2 \sin^2 \theta) (y \sin \theta - y' \cos \theta) d\theta$$

Therefore, the original liquid height "h" is

$$h = \frac{V_{\ell}}{\pi} \int_0^{\theta_1} (1 - y^2 \sin^2 \theta) (y \sin \theta - y' \cos \theta) d\theta \quad (14B)$$

4. Special Boundary Conditions Applicable to a Cylinder - Since the liquid fill level has no significance in the calculation of interface shape in cylinders, the only requirement for the observation point position (coordinate system origin) is that it be above the interface. Therefore, the distance to the low gravity face can be set equal to one, that is, $y_0 = 1$, and the initial conditions for the main interface differential equation (equation (37)) can be simplified to

$$\begin{aligned} y(0) &= y_0 = 1 \\ y'(0) &= 0 \\ y'' &= 1 - K_0 \end{aligned} \quad (15B)$$

APPENDIX C

COMPUTER PROGRAM FOR DETERMINING INTERFACE SHAPE

A. General Computer Procedure

A general outline of the computer program sequence in engineering terms is as follows:

1. Print out input data which includes:

COMPUTER SYMBOL	ENGINEERING SYMBOL	DEFINITION	UNITS
KSVHC		Container Designation: 1 - Spherical 2 - Vertical 3 - Oblate Spheroid 4 - Prolate Spheroid	
B	B_N	Bond Number	Dimensionless
YG	y_g	Distance from Origin to Surface for Bond Number = ∞	Dimensionless
A2		Spheroidal Container Major Axis	Dimensionless
B2		Spheroidal Container Minor Axis	Dimensionless
CONANG	α	Contact Angle	Degrees
Y_o^{**}	y_o	Estimated Distance from Origin to Low Gravity Surface Center Point	Dimensionless

2. The input data are used as initial values in the "Runge-Kutta" iteration solution of the main differential equation (33), which continues until the

* The authors wish to acknowledge the contributions of Mrs Pam T. Hughes, of Computer Sciences Corporation, to the development of the computer program outlined herein.

** After some experience has been acquired in determining interface shapes, initial values of y_o can be determined that will enable more rapid computer convergence. Also, note that $y_o = 1$ in the case of a cylinder, since fill level has no influence on interface (see Appendix B).

interface intersects the container boundary. The Runge-Kutta formulas applied are those specified in Reference 11 for the integration of second-order equations of the general type,

$$y'' = f(\theta, y, y')$$

and consist of

$$k_1 = \Delta\theta f(\theta_n, y_n, y_n')$$

$$k_2 = \Delta\theta f\left(\theta_n + \frac{\Delta\theta}{2}, y_n + \frac{\Delta\theta}{2} y_n' + \frac{\Delta\theta}{8} k_1, y_n' + \frac{k_1}{2}\right)$$

$$k_3 = \Delta\theta f\left(\theta_n + \frac{\Delta\theta}{2}, y_n + \frac{\Delta\theta}{2} y_n' + \frac{\Delta\theta}{2} k_1, y_n' + \frac{k_2}{2}\right)$$

$$k_4 = \Delta\theta f(\theta_n + \Delta\theta, y_n + \Delta\theta y_n' + \frac{\Delta\theta}{2} k_3, y_n' + k_3)$$

$$\Delta y = \Delta\theta + \frac{1}{6} (k_1 + k_2 + k_3)$$

$$\Delta y' = \frac{1}{6} (k_1 + 2k_2 + 2k_3 + k_4)$$

3. Solve for interface/container boundary contact angle, α , and compare with the desired contact angle. If the calculated contact angle is negative, K_0 is too large and must be decreased. However, if the angle is positive but too large, it is necessary to increase K_0 . In either case, new values of K_0 are selected and used as new input in the Runge-Kutta solution until the desired contact angle is approached.

4. Empty fraction* (vapor volume/container volume), β , is determined and compared with the desired empty fraction. If the correct β is not calculated, the value of y_0 determined is entered in step 1, and new β is computed. This procedure is continued until enough data is generated to extrapolate or interpolate a curve fit of " y_0 versus β " for the correct y_0 .

5. The correct value of y_0 is entered in step 1 with the original value of K_0 , and the entire procedure is repeated until the desired contact angle and empty fraction are obtained.

* In the case of a cylinder, the empty fraction criteria is by-passed.

6. Program output data is printed:

COMPUTER SYMBOL	ENGINEERING SYMBOL	DEFINITION	UNITS
X/R; OX	X/R_0	Horizontal Distance from Container Vertical Axis to Liquid-Vapor Interface	Dimensionless
Z/R; OZ	Z/R_0	Vertical Distance from X Axis to Liquid-Vapor Interface	Dimensionless
ANG; CONTACT ANGLE		Contact Angle	Degrees
DXDY	K_0	Parameter Related to Curvature at Interface Centerpoint	Dimensionless
YO	y_0	Distance from Origin to Low Gravity Surface Centerpoint	Dimensionless
TH; THETA	θ	Angle Measured from Vertical Axis to y	Degrees
BETA; EMPTY FRACTION		Calculated Empty Fraction	Dimensionless
BETAD	D	Desired Empty Fraction	Dimensionless
Y	y	Distance from Origin to Liquid Surface	Dimensionless

B. Program Limitations

As the low gravity interface shapes approach flatness at high Bond numbers, increasingly accurate values of K_0 are required because K_0 is approaching zero. In the present program, difficulty is encountered in obtaining contact angles of less than approximately five degrees at Bond numbers greater than or equal to 200, because the computer (GE 235) is unable to store the very small variations of K_0 required for further convergence. This problem could be eliminated by using a more accurate computer (IBM 7094) if interface shapes at very high Bond numbers are desired; however, the interface shape variation caused by a five-degree contact angle deviation at Bond numbers above 150 is insignificant for most applications.

C. Programming Information

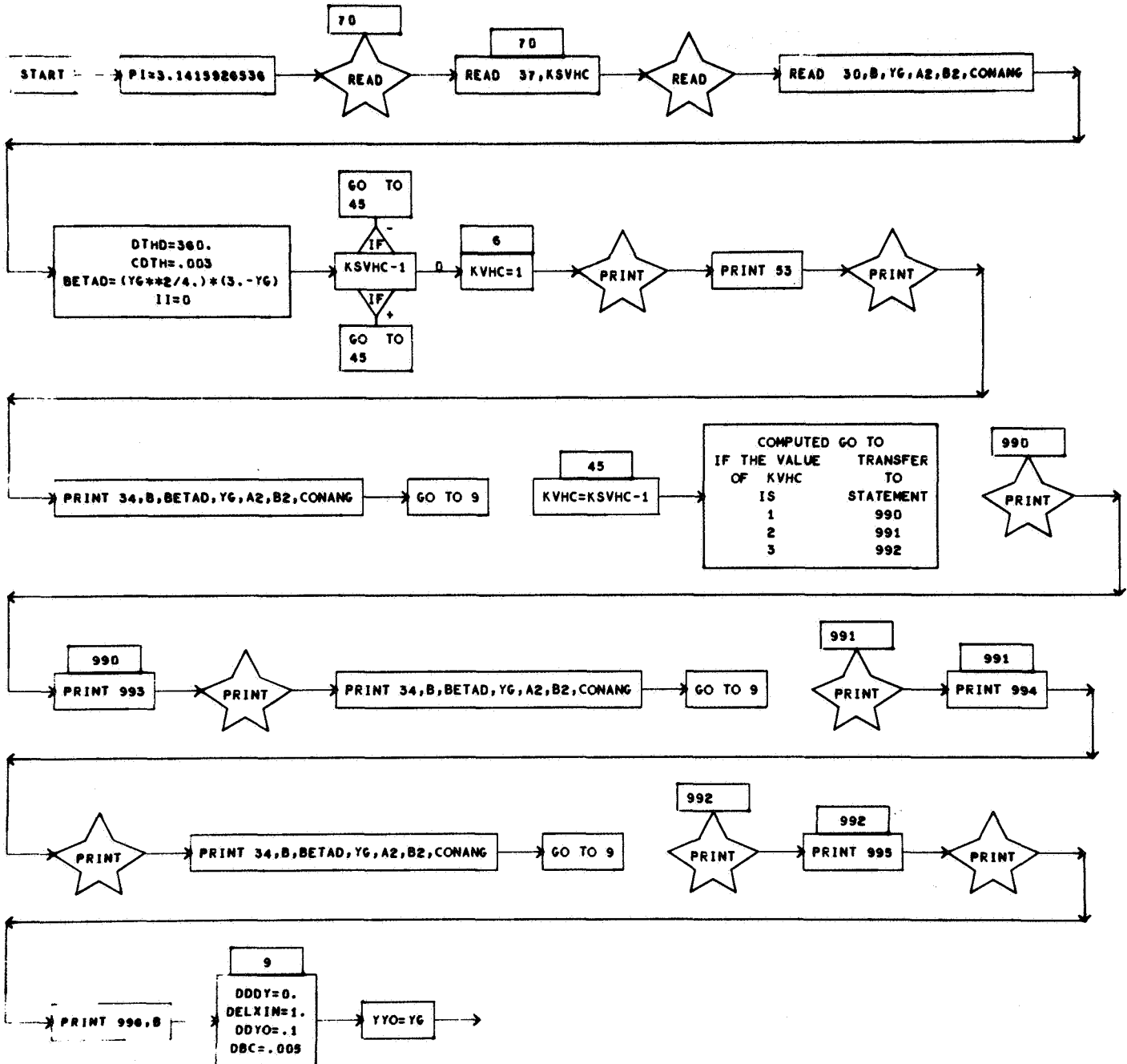
1. Definition of Terms - Some of the significant terms not defined previously include:

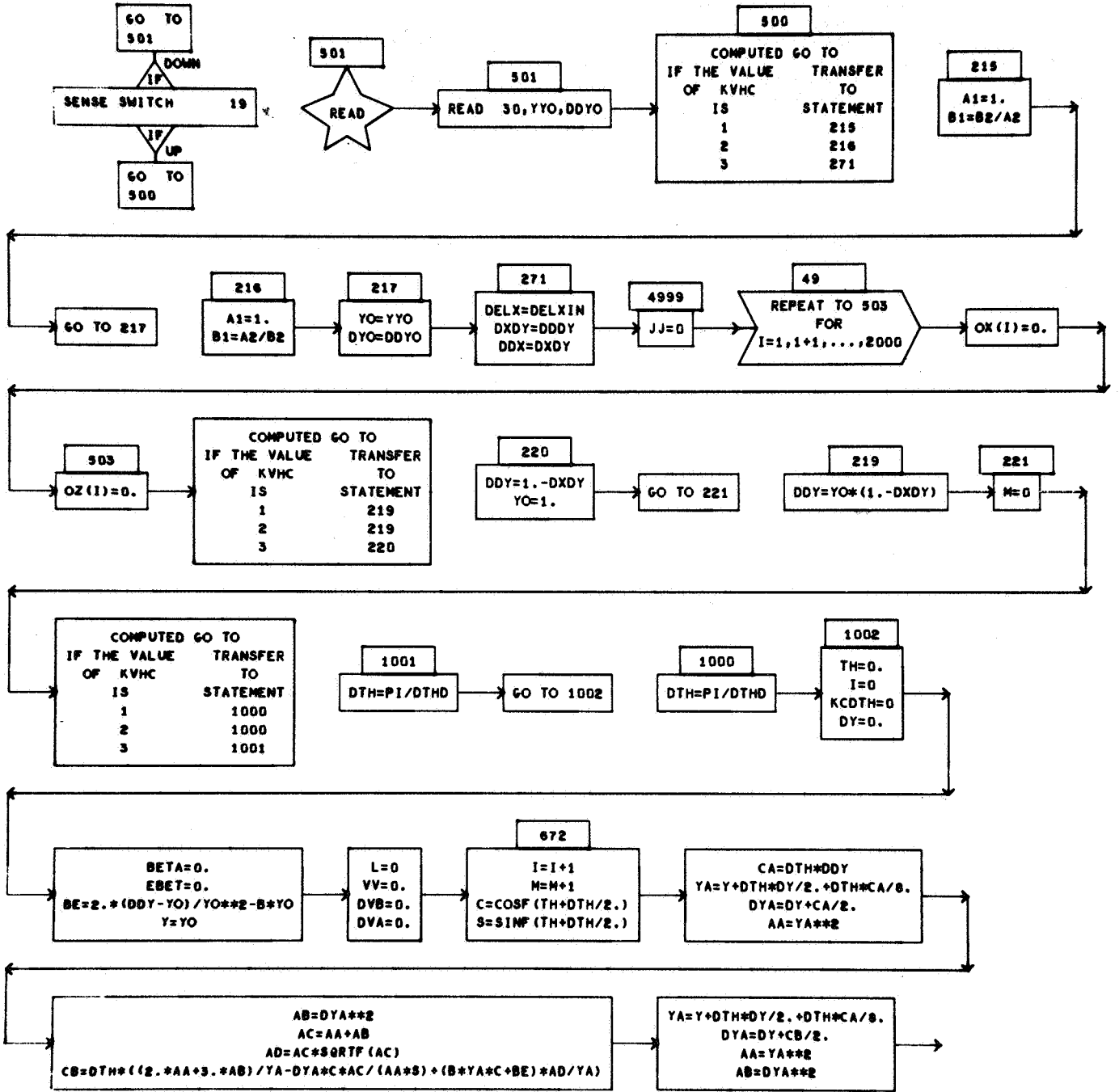
COMPUTER SYMBOL	ENGINEERING SYMBOL	DEFINITION	UNITS
DDY	y''	Second Derivative of y with Respect to θ	Dimensionless
DY	y'	First Derivative of y with Respect to θ	Dimensionless
S	$\sin \theta$	$\sin \theta$	Dimensionless
C	$\cos \theta$	$\cos \theta$	Dimensionless
VV	V_L	Liquid Volume	Dimensionless
DVB	ΔV_L	Incremental Liquid Volume	Dimensionless
DBET	$\Delta \beta$	Incremental Empty Fraction	Dimensionless

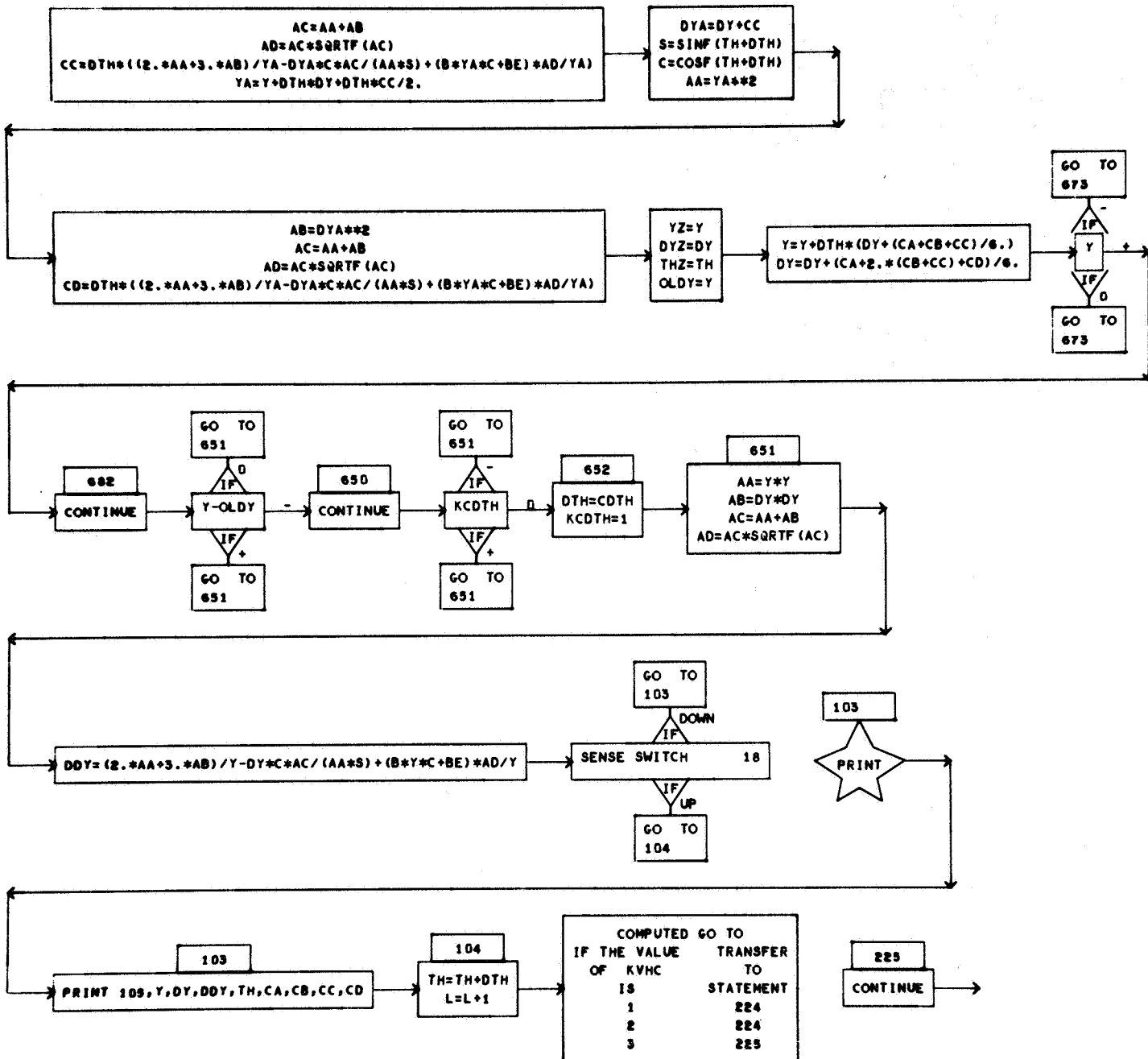
2. Flow Chart

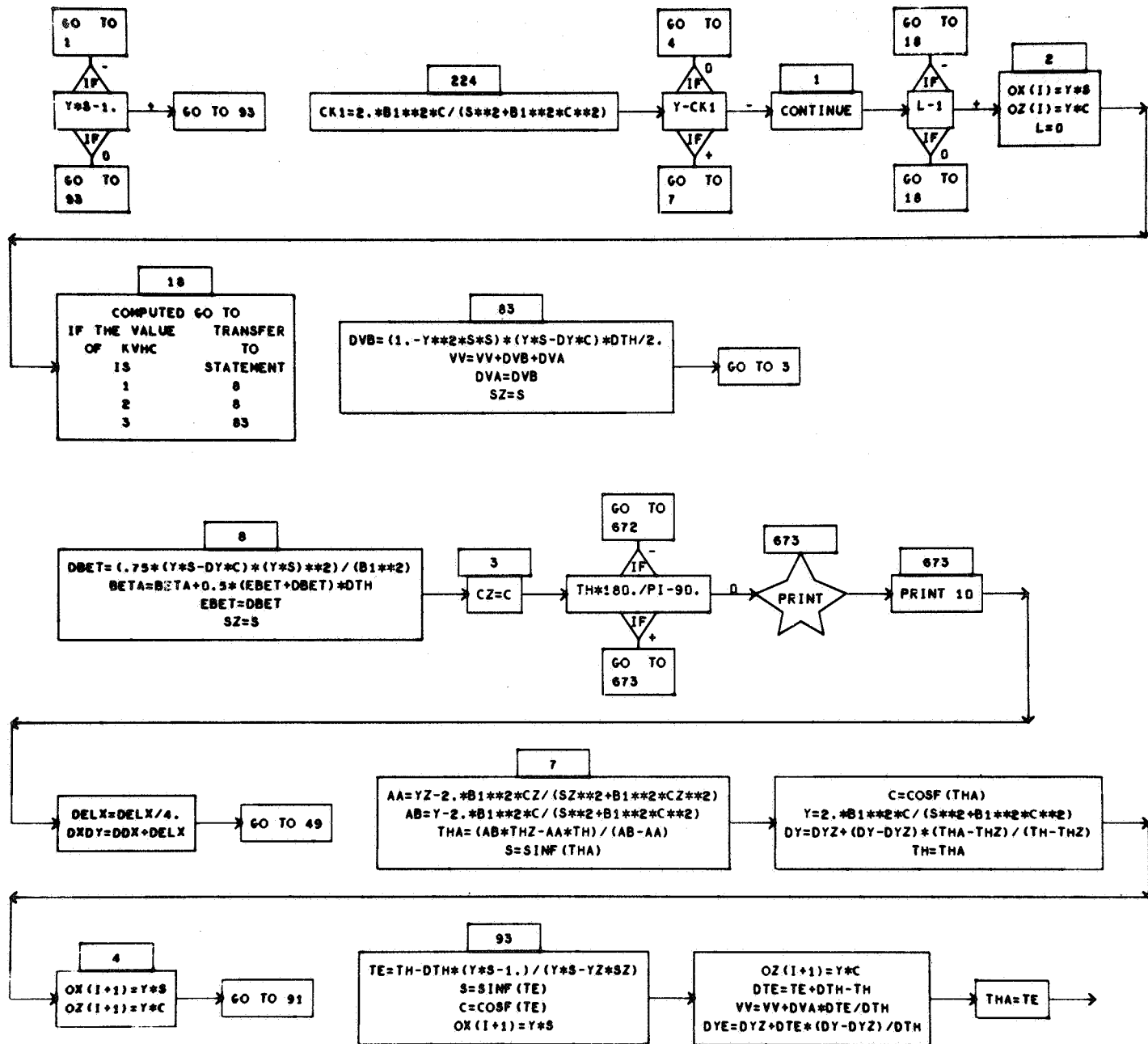
KOMMON OX(2000),OZ(2000)

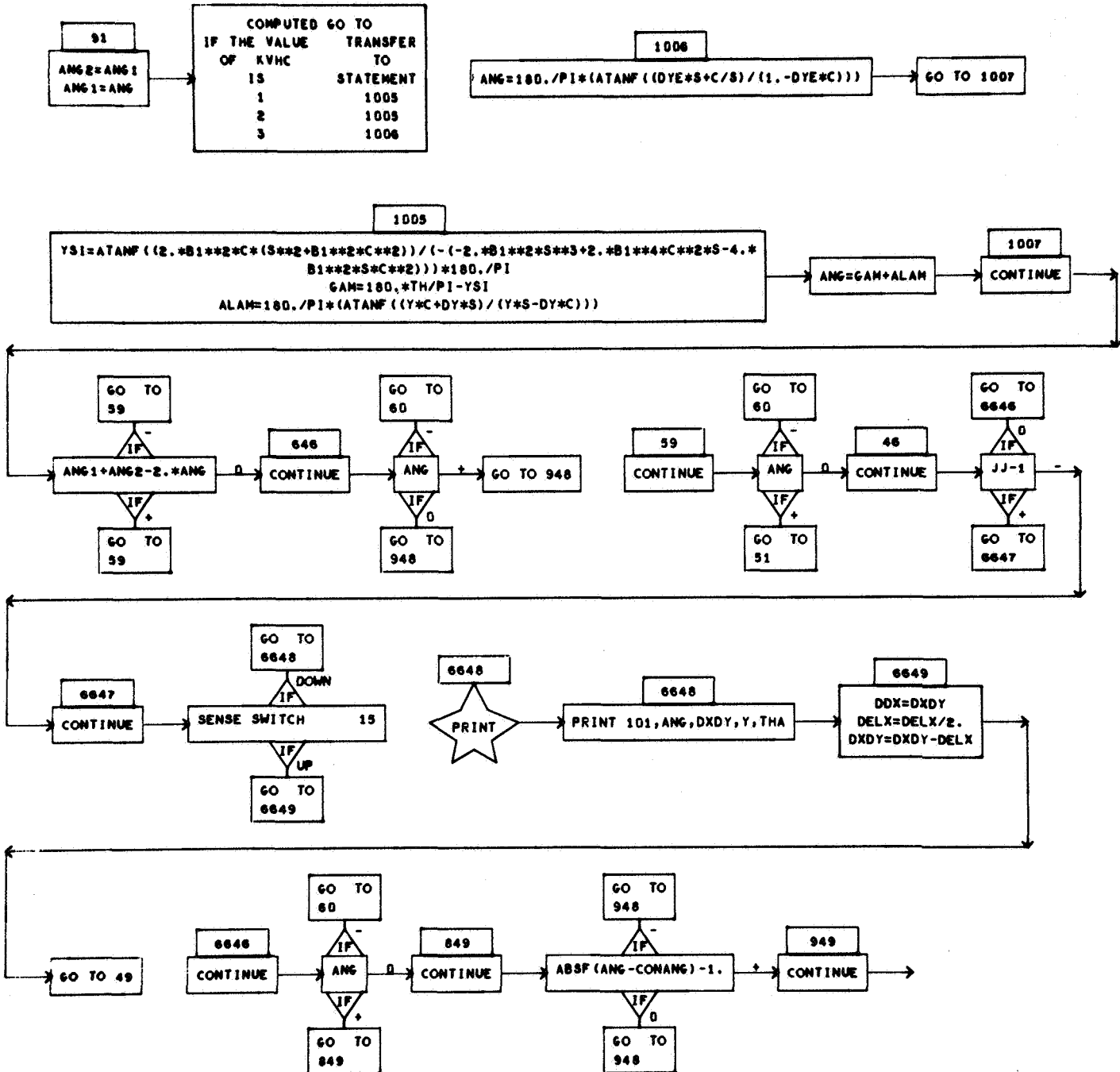
PAGE 1

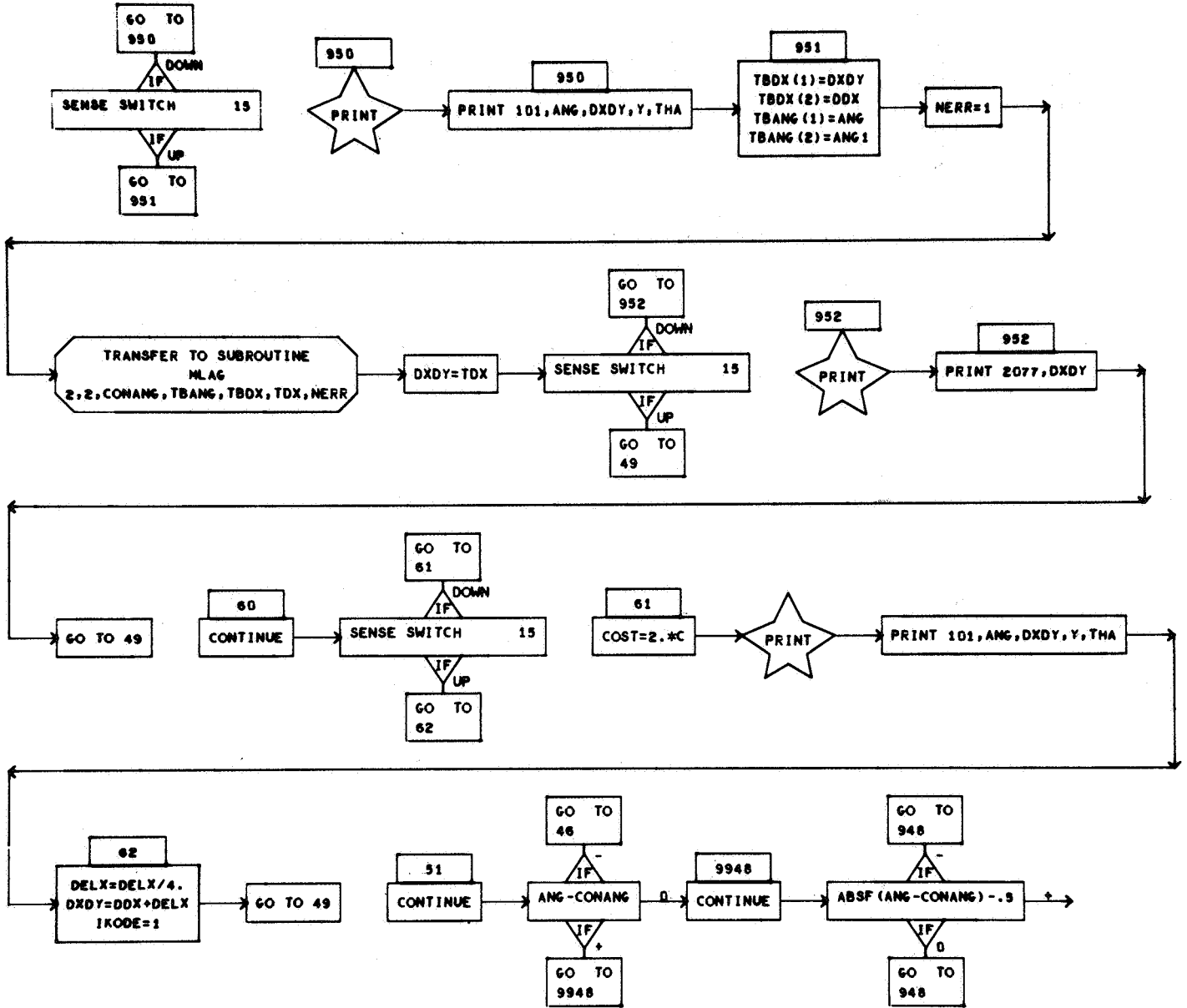


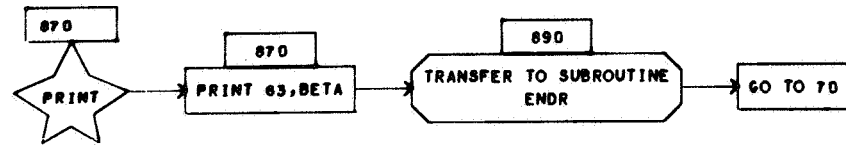
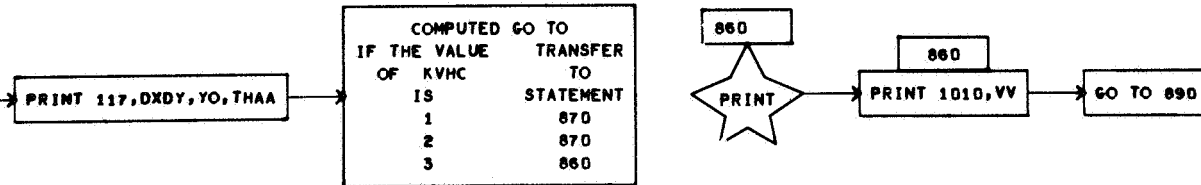
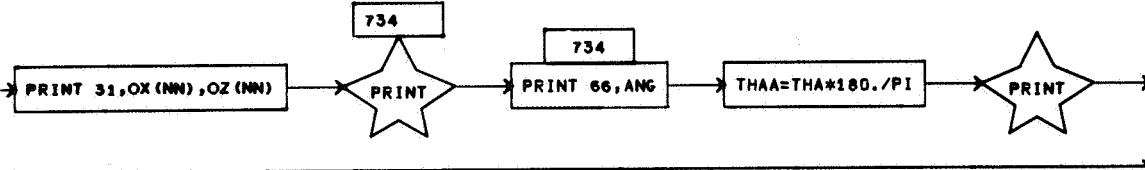
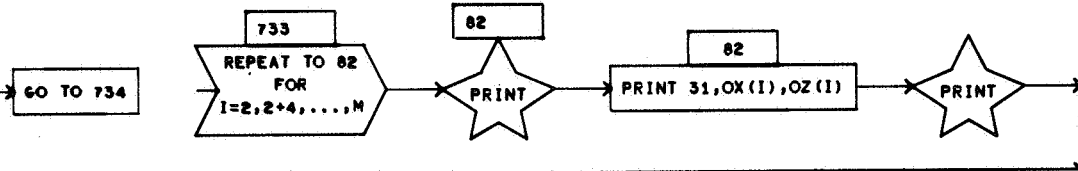
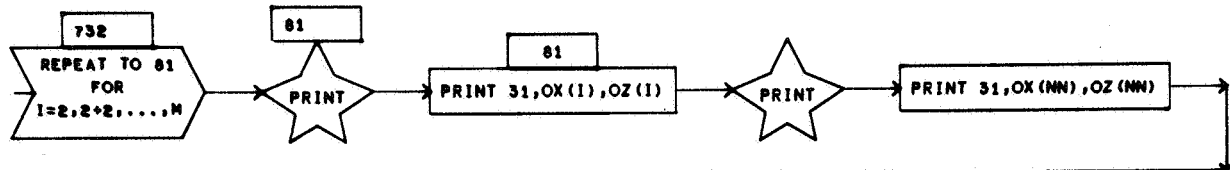
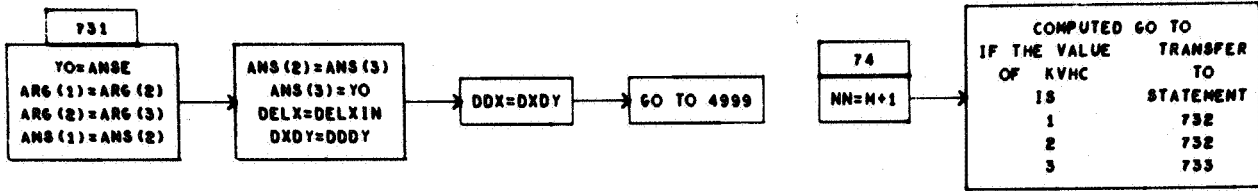












3. Program Listing

```
C    SPHERE INTERFACE, EMPIRICAL - VFRSION C-2
      KOMMON OX(2000),OZ(2000)
      COMMON ANS(3),ARG(3),TRDX(2),TBANG(2)
29  FORMAT (I2)
30  FORMAT (5E16.8)
31  FORMAT (6HX/R = ,F7.4,8H, Z/R = ,F7.4)
10  FORMAT (5X,10HNO CONTACT)
66  FORMAT (14HCONTACT ANGLF ,F7.3,8H DFGRFES)
34  FORMAT( //,1X3HB= E11.5,3X6HBETAD=E11.5,3X3HYG=E11.5,3X3HA= F11.5,
      13X3HB= E11.5,2X11HANG DESIRED,2XF11.5)
53  FORMAT (1H1,1X27HSPHERE INTERFACE, EMPIRICAL)
63  FORMAT (17HEMPTY FRACTION = ,F6.4)
993 FORMAT(1H1,16HPROLATE SPHEROID)
994 FORMAT(1H1,15HOBLATE SPHEROID)
995 FORMAT(1H1,8HCYLINDER)
996 FORMAT(/2HR=F11.5)
      PI=3.1415926536
70  READ 37,KSVHC
      READ 30,B,YG,A2,B2,CONANG
      DTHD=360.
      CDTH=.003
      BETAD=(YG**2/4.)*(3.-YG)
      II=0
      IF(KSVHC-1)45,6,45
6    KVHC=1
      PRINT 53
      PRINT 34,B,BETAD,YG,A2,B2,CONANG
      GO TO 9
45  KVHC=KSVHC-1
      GO TO(990,991,992),KVHC
990 PRINT 993
      PRINT 34,B,BETAD,YG,A2,B2 ,CONANG
      GO TO 9
991 PRINT 994
      PRINT 34,B,BETAD,YG,A2,B2 ,CONANG
      GO TO 9
992 PRINT 995
      PRINT 996,B
9    DDDY=0.
      DFLXIN=1.
      DDYO=.1
      DBC=.005
      YYO=YG
37  FORMAT(I1)
      IF(SENSE SWITCH 19)501,500
501 READ 30,YYO,DDYO
500 GO TO (215,216,271),KVHC
215 A1=1.
      B1=B2/A2
      GO TO 217
216 A1=1.
      B1=A2/B2
217 YO=YYO
      DY0=DDYO
271 DELX=DELXIN
      DXDY=DDDY
      DDX=DXDY
4999 JJ=0
```

```

49 DO 503 I=1,2000
   OX(I)=0.
503 OZ(I)=0.
   GO TO (219,219,220),KVHC
220 DDY=1.-DXDY
   YO=1.
   GO TO 221
219 DDY=YO*(1.-DXDY)
221 M=0
   GO TO (1000,1000,1001),KVHC
1001 DTH=PI/DTHD
   GO TO 1002
1000 DTH=PI/DTHD
1002 TH=0.
   I=0
   KCDTH=0
   DY=0.
   BETA=0.
   FBET=0.
   RE=2.*(DDY-YO)/YO**2-R*YO
   Y=YO
   L=0
   VV=0.
   DVR=0.
   DVA=0.
672 I=I+1
   M=M+1
   C=COSF(TH+DTH/2.)
   S=SINF(TH+DTH/2.)
   CA=DTH*DDY
   YA=Y+DTH*DY/2.+DTH*CA/8.
   DYA=DY+CA/2.
   AA=YA**2
   AB=DYA**2
   AC=AA+AB
   AD=AC*SQRTF(AC)
   CB=DTH*((2.*AA+3.*AB)/YA-DYA*C*AC/(AA*S)+(B*YA*C+RE)*AD/YA)
   YA=Y+DTH*DY/2.+DTH*CA/8.
   DYA=DY+CB/2.
   AA=YA**2
   AB=DYA**2
   AC=AA+AB
   AD=AC*SQRTF(AC)
   CC=DTH*((2.*AA+3.*AB)/YA-DYA*C*AC/(AA*S)+(B*YA*C+RE)*AD/YA)
   YA=Y+DTH*DY+DTH*CC/2.
   DYA=DY+CC
   S=SINF(TH+DTH)
   C=COSF(TH+DTH)
   AA=YA**2
   AB=DYA**2
   AC=AA+AB
   AD=AC*SQRTF(AC)
   CD=DTH*((2.*AA+3.*AB)/YA-DYA*C*AC/(AA*S)+(B*YA*C+RE)*AD/YA)
   YZ=Y
   DYZ=DY
   THZ=TH
   OLDY=Y
   Y=Y+DTH*(DY+(CA+CB+CC)/6.)

```

```

        DY=DY+(CA+2.*(CB+CC)+CD)/6.
        IF(Y)673,673,682
682 IF(Y-OLDY)650,651,651
650 IF(KCDTH)651,652,651
652 DTH=CDTH
        KCDTH=1
651 AA=Y*Y
        AB=DY*DY
        AC=AA+AB
        AD=AC*SQRTE(AC)
        DDY=(2.*AA+3.*AB)/Y-DY*C*AC/(AA*S)+(B*Y*C+BE)*AD/Y
        IF (SENSF SWITCH 18)103,104
103 PRINT 105,Y,DY,DDY,TH,CA,CB,CC,CD
105 FORMAT(5X,8F12.5)
104 TH=TH+DTH
        L=L+1
        GO TO (224,224,225),KVHC
225 IF(Y*S-1.)1,93,93
224 CK1=2.*B1**2*C/(S**2+B1**2*C**2)
        IF(Y-CK1)1,4,7
    1 IF(L-1)18,18,2
    2 OX(I)=Y*S
        OZ(I)=Y*C
        L=0
18 GO TO (8,8,83),KVHC
83 DVB=(1.-Y**2*S*S)*(Y*S-DY*C)*DTH /2.
        VV=VV+DVB +DVA
        DVA=DVB
        SZ=S
        GO TO 3
    8 DBET=(.75*(Y*S-DY*C)*(Y*S)**2)/(B1**2)
        BETA=BETA+0.5*(EBET+DBET)*DTH
        EBET=DBET
        SZ=S
    3 CZ=C
        IF(TH*180./PI-90.)672,673,673
673 PRINT 10
        DELX=DELX/4.
        DXDY=DDX+DELX
        GO TO 49
    7 AA=YZ-2.*B1**2*CZ/(SZ**2+B1**2*CZ**2)
        AB=Y-2.*B1**2*C/(S**2+B1**2*C**2)
        THA=(AB*THZ-AA*TH)/(AB-AA)
        S=SINF(THA)
        C=COSF(THA)
        Y=2.*B1**2*C/(S**2+B1**2*C**2)
        DY=DYZ+(DY-DYZ)*(THA-THZ)/(TH-THZ)
        TH=THA
    4 OX(I+1)=Y*S
        OZ(I+1)=Y*C
        GO TO 91
93 TE=TH-DTH*(Y*S-1.)/(Y*S-YZ*SZ)
        S=SINF(TE)
        C=COSF(TE)
        OX(I+1)=Y*S
        OZ(I+1)=Y*C
        DTE=TE+DTH-TH
        VV=VV+DVA*DTE/DTH

```

```

DYE=DYZ+DTE*(DY-DYZ)/DTH
THA=TE
91 ANG2=ANG1
   ANG1=ANG
   GO TO (1005,1005,1006),KVHC
1006 ANG=180./PI*(ATANF((DYE*S+C/S)/(1.-DYE*C)))
   GO TO 1007
1005 YSI= ATANF((2.*B1**2*C*(S**2+P1**2*C**2))/(-(-2.*B1**2*S**3+
12.*B1**4*C**2*S-4.*B1**2*S*C**2)))*180./PI
   GAM=180.*TH/PI-YSI
   ALAM=180./PI*(ATANF((Y*C+DY*S)/(Y*S-DY*C)))
   ANG=GAM+ALAM
1007 IF(ANG1+ANG2-2.*ANG)59,646,59
   646 IF(ANG)60,948,948
   59 IF (ANG) 60,46,51
   46 IF(JJ-1)6647,6646,6647
6647 IF(SENSE SWITCH 15)6648,6649
6648 PRINT 101,ANG,DXDY,Y,THA
6649 DDX=DXDY
   DELX=DELX/2.
   DXDY=DXDY-DELX
   GO TO 49
6646 IF(ANG)60,849,849
   849 IF(ABSF(ANG-CONANG)-1.)948,948,949
   949 IF(SENSE SWITCH 15)950,951
   950 PRINT 101,ANG,DXDY,Y,THA
   951 TBDX(1)=DXDY
   TBDX(2)=DDX
   TBANG(1)=ANG
   TBANG(2)=ANG1
   NERR=1
   CALL MLAG(2,2,CONANG,TBANG,TBDX,TDX,NERR)
   DXDY=TDX
   IF(SENSE SWITCH 15)952,49
   952 PRINT 2077,DXDY
2077 FORMAT(1X4HDXDYE16.8)
   GO TO 49
   60 IF (SENSE SWITCH 15) 61,62
   61 COST=2.*C
   PRINT 101,ANG,DXDY,Y,THA
   62 DELX=DELX/4.
   DXDY = DDX + DELX
   IKODE=1
   GO TO 49
   51 IF(ANG-CONANG)46,9948,9948
9948 IF(ABSF(ANG-CONANG)-.5)948,948,52
   52 COST=2.*C
   IF(IKODE)852,853,852
   852 DELX=DELX/4.
   IKODE=0
   853 CONTINUE
   JJ=1
   IF(SENSE SWITCH 15)854,855
   854 PRINT 101,ANG,DXDY,Y,THA
   101 FORMAT(1X3HANGE12.5,2X4HDXDYE16.8,2X1HYE12.5,2X2HTHE12.5)
855 DDX = DXDY
   DXDY = DXDY + DELX
   GO TO 49

```

```

948 GO TO (850,850,74 ),KVHC
850 SS=S*S
    DBET=(.75*(Y*S-DY*C)*(Y*S)**2)/(B1**2)
    ZZZ=-OZ(I+1)
    BETA=BETA+0.5*(EBET+DBET)*(TH-THZ)+(3./4.*(ZZZ**3/3.+ZZZ**2))
    RB=BETAD-BETA
    YO1=YO
    PRINT 667,BETA,YO
667 FORMAT(1X4HBETAE16.8,3X2HYOE12.5)
    IF(ABSF(RB)-DBC )74,74,47
47 NERR=1
    IF(II)32,33,32
33 II=II+1
    ANS(1)=YO
    YO=YO+DYO
    ARG(1)=BETA
    DELX=DELXIN
    DXDY=DDDY
    DDX=DXDY
    GO TO 4999
32 IF(II-1)35,36,35
36 II=II+1
    ANS(2)=YO
    ARG(2)=BETA
    YO=YO+DYO
    DELX=DELXIN
    DXDY=DDDY
    DDX=DXDY
    GO TO 4999
35 IF(II-2)39,38,39
38 ANS(3)=YO
    II=II+1
39 ARG(3)=BETA
    IF(ARG(1)-ARG(3))78,58,58
58 AT=ARG(1)
    ARG(1)=ARG(3)
    ARG(3)=AT
    TS=ANS(1)
    ANS(1)=ANS(3)
    ANS(3)=TS
78 IF(ARG(1)-ARG(2))87,88,88
88 PP=ARG(1)
    ARG(1)=ARG(2)
    ARG(2)=PP
    TS=ANS(1)
    ANS(1)=ANS(2)
    ANS(2)=TS
87 IF(ARG(2)-ARG(3))89,90,90
90 ST=ARG(2)
    ARG(2)=ARG(3)
    ARG(3)=ST
    TS=ANS(2)
    ANS(2)=ANS(3)
    ANS(3)=TS
89 NERR=1
    CALL MLAG(3,3,BETAD,ARG,ANS,ANSE,NERR)
    PRINT 9101,ANSE
9101 FORMAT(1X16HEXTRAPOLATED YO E12.5)

```

```

IF (ANSE) 730, 730, 731
730 DYO=DYO+DDYO/2.
DELX=DELXIN
DXDY=DDDY
DDX=DXDY
II=0
YO=YYO
GO TO 4999
731 YO=ANSE
ARG(1)=ARG(2)
ARG(2)=ARG(3)
ANS(1)=ANS(2)
ANS(2)=ANS(3)
ANS(3)=YO
DFLX = DFLXIN
DXDY=DDDY
DDX=DXDY
100 FORMAT(1X2E16.8)
GO TO 4999
74 NN=M+1
GO TO (732,732,733),KVHC
732 DO 81 I=2,M,2
81 PRINT 31,OX(I),OZ(I)
PRINT 31,OX(NN),OZ(NN)
GO TO 734
733 DO 82 I= 2,M ,4
82 PRINT 31,OX(I),OZ(I)
PRINT 31,OX(NN),OZ(NN)
734 PRINT 66,ANG
THAA=THA*180./PI
PRINT 117,DXDY,YO,THAA
GO TO (870,870,860),KVHC
860 PRINT 1010,VV
1010 FORMAT(2X7HHEIGHT=E12.5)
GO TO 890
870 PRINT 63,BETA
117 FORMAT(2X5HDXDY=E16.8,3HYO=E16.8,2X6HTHETA= E16.8)
890 CALL ENDR
GO TO 70
END

```

D. Deck Setup

1. Computer Configuration

a.. Computer	GE-235
b. Core size required	16 K
c. Language	F II
d. System	SLEM
e. Plotter required	NONE
f. Card punch required	NONE

2. Estimated Run Time - Five minutes

3. Restart Procedure - Multiple Cases Read by ENDR

4. Deck Sequence

ZERO MEMORY 16 K
SLEM CALL CARD
ID CARD
BINARY FOR MAIN DECK
BINARY FOR MLAG
BINARY FOR ENDR
1/2 PUNCH
DATA INPUT DECK

5. Diagonistics

If the program seems to be cycling, the program can be run with sense switch 15 down and the computer will print out the calculated contact angle, DXDY, and YO after each pass through the Runge-Kutta procedure.

6. Input Sheet

INPUT DATA SHEET

Date: _____

Job No. 574260

KSVHC = 1, 2, 3, 4

Card 1

1 - Spherical Shape, 2 - Vertical ellipse,
3 - Horizontal ellipse, 4 - Cylinder

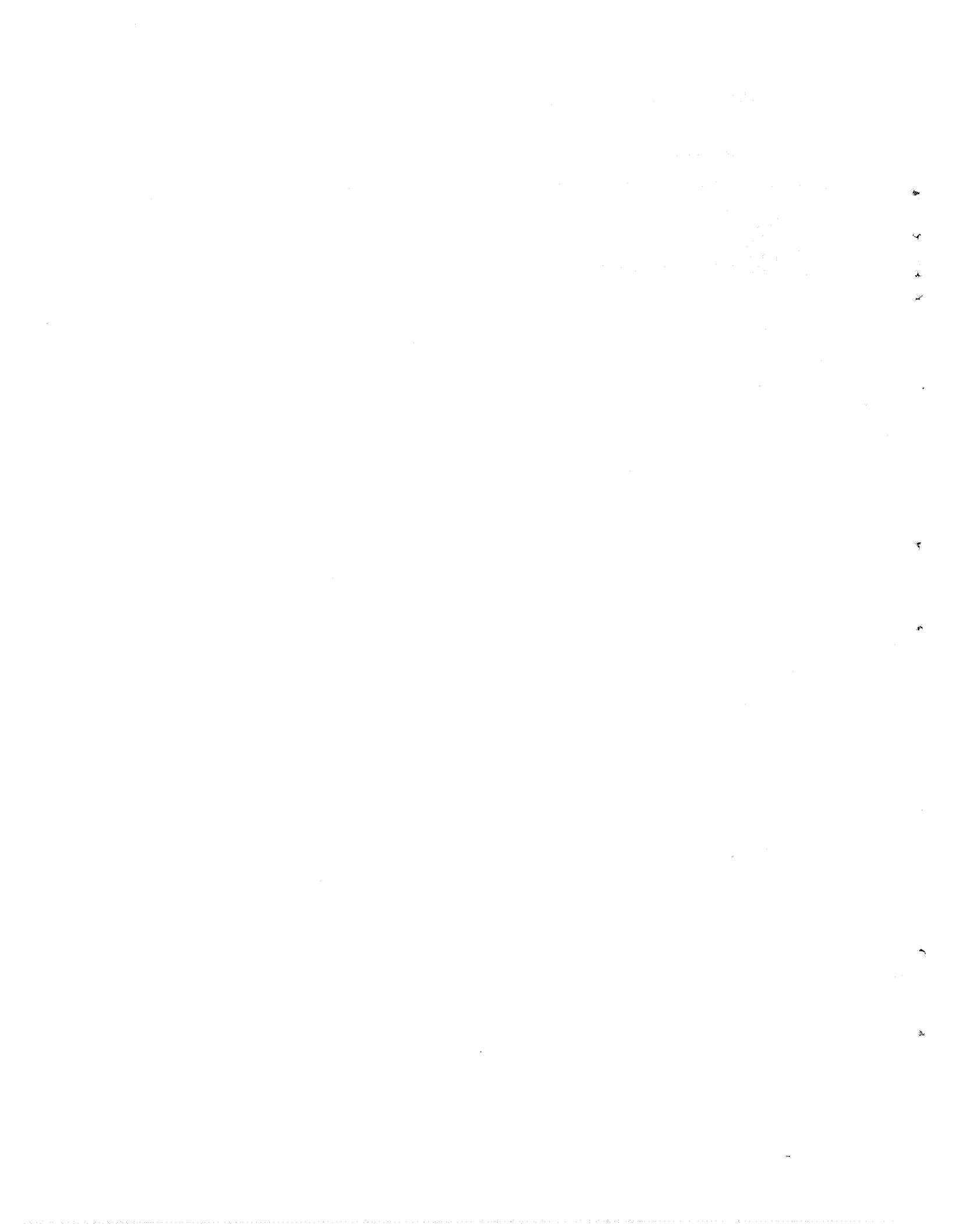
Card 2

Bond No.	YG - Fill Level	A ₂ - Major Axis	B ₂ - Minor Axis	Contact Angle
Col 1 16 17	32 33	48 49	64 65	80

Card 3

OPTIONAL

Y ₀	DY ₀
Col 1 16 17	32



REFERENCES

1. Maxwell, J. C.: "Capillary Action." Encyclopedia Britannica, 9th ed., 1878.
2. Davies, J. T.; and Rideal, E. K.: Interfacial Phenomena. Academic Press, New York and London, 1963, pp. 1-3.
3. Adam, N. K.: The Physics and Chemistry of Surfaces. Oxford University Press, London, 1941, p. 3.
4. Adamson, A. W.: Physical Chemistry of Surfaces. Interscience Publishers, New York, 1960, p. 4.
5. Satterlee, H. M.; and Chin, J. L.: "Meniscus Shape Under Reduced Gravity Conditions." Symposium on Fluid Mechanics and Heat Transfer Under Low Gravitational Conditions, Lockheed Missiles and Space Company, June 24 - 25, 1965.
6. Jahsman, W. E.: "The Equilibrium Shape of the Surface of a Fluid in a Cylindrical Tank." Developments in Mechanics, Vol. 1, Edited by J. E. Lay and L. E. Melvern, Plenum Press, New York, 1961, pp. 603-612.
7. Geiger, F. W.: "Hydrostatics of a Fluid in a Cylindrical Container at Low Bond Numbers." Brown Engineering Company, Inc., Technical Note R-207, July 1966.
8. Bashforth, F.; and Adams, J. C.: An Attempt to Test the Theories of Capillary Action by Comparing the Theoretical and Measured Forms of Drops of Fluid. University Press, Cambridge, England, 1883.
9. Reynolds, W. C.; Saad, M. A.; and Satterlee, H. M.: "Capillary Hydrostatics and Hydrodynamics at Low g." Technical Report No. LG-3, Mechanical Engineering Department, Stanford University, September 1, 1964.
10. Li, T.: "Hydrostatics in Various Gravitational Fields." Journal of Chemical Physics, Vol. 36, No. 9, May 1, 1962, pp. 2369-2375.

11. Yeh, G. C. K.; and Hutton, R. E.: "Static Configurations in an Axisymmetric Tank in Various Gravitational Fields." TRW Space Technology Laboratories, Report EM15-2 (9840-6010-RU000), March 1965.
12. Journey, W. H.: "The Configuration of a Contained Liquid in a Constant Gravitational Field." Martin-Marietta Corporation, Denver Division, TM 0444-65-4, October 1965.
13. Sokolnikoff, I. S.; and Redheffer, R. M.: Mathematics of Physics and Modern Engineering. McGraw Hill Book Company, Inc., New York, 1958, p. 267.
14. Wood, G. B.: "Zero-G Report-Liquid-Liquid Model." General Dynamics/Astronautics Division of Convair Report 55D859-9, May 1962.
15. Scarborough, J. B.: Numerical Mathematical Analysis. The Johns Hopkins Press, Baltimore, 1962, p. 358.
16. Chin, J. H., et al: "Analytical and Experimental Study of Liquid Orientation and Stratification in Standard and Reduced Gravity Fields." Lockheed Missiles and Space Company Report No. 2-05-64-1, July 1964.
17. Masica, W. J., et al: "Hydrostatic Stability of the Liquid-Vapor Interface in a Gravitational Field." NASA TND-2267, May 1964.
18. Barksdale, T. R.; and Paynter, H. L.: "Design, Fabrication, and Testing of Subscale Propellant Tanks with Capillary Traps." Martin-Marietta Corp. Monthly Progress Report for Contract NAS8-20837, August 1967.
19. Paynter, H. L.: "Time for a Totally Wetting Liquid to Deform from a Gravity-Dominated to a Nulled-Gravity Equilibrium State." AIAA Journal, Vol. 2, No. 9, December 1964, p. 1627.
20. Fung, F. W.: "Dynamic Response of Liquids in Partially Filled Containers Suddenly Experiencing Weightlessness." Symposium on Fluid Mechanics and Heat Transfer Under Low Gravitational Conditions, Lockheed Missiles and Space Company, June 24 - 25, 1965.
21. Siegret, C. E.; Petrash, D. A.; and Otto, E. W.: "Time Response of Liquid-Vapor Interface After Entering Weightlessness." NASA TN D-2458, 1964.

22. Young, T.: "An Essay on the Cohesion of Fluids." *Philosophical Transactions of the Royal Society of London*, Vol. 95, 1805, p. 65.
23. Bikerman, J. J.: "Solid Surfaces." *Second International Congress of Surface Activity*, Vol. III, Academic Press, New York, 1957, p. 131.
24. Johnson, R. E.: "Conflicts Between Gibbsian Thermodynamics and Recent Treatments of Interfacial Energies in Solid-Liquid-Vapor Systems." *Journal of Physical Chemistry*, Vol. 63, October 1959, pp. 1655-1658.
25. Lester, G. R.: "Contact Angles of Liquids at Deformable Solid Surfaces." *Journal of Colloid Science*, Vol. 16, 1961, pp. 315-326.
26. Wenzel, R. M.: "Resistance of Solid Surfaces to Wetting by Water." *Industry and Chemical Engineering*, Vol. 28, 1936, pp. 988-994.
27. Langmuir, I.: "The Mechanism of the Surface Phenomena of Flotation." *Transactions of the Faraday Society*, Vol. 15, Part III, 1919, p. 62.
28. "Contact Angle, Wettability, and Adhesion." *Kendal Award Symposium Proceedings at the 144th Meeting of the American Chemical Society*, Los Angeles, April 2 - 3, 1963.
29. Mainardi, P.: Calculus and its Applications. Pergamon Press, Inc., New York, 1963, p. 168.

October 7, 1968

APPROVAL

TM X-53790

LOW GRAVITY LIQUID-VAPOR INTERFACE
SHAPES IN AXISYMMETRIC CONTAINERS
AND A COMPUTER SOLUTION

By Leon J. Hastings and Reginald Rutherford, III

The information in this report has been reviewed for security classification. Review of any information concerning Department of Defense or Atomic Energy Commission programs has been made by the MSFC Security Classification Officer. This report, in its entirety, has been determined to be unclassified.

This document has also been reviewed and approved for technical accuracy.



A. L. WORLUND
Chief, Fluid Mechanics Section



G. D. HOPSON
Chief, Fluid-Thermal Systems Branch



H. G. PAUL
Chief, Propulsion Division



W. R. LUCAS
Director, Propulsion and Vehicle Engineering Laboratory

DISTRIBUTION

DIR	Dr. von Braun
DEP-T	Dr. Rees
I-DIR	General O'Connor
	Dr. Mrazek
R-DIR	Mr. Weidner
R-AS-DIR	Mr. Williams
R-RP-DIR	Dr. Stuhlinger
R-AERO-DIR	Dr. Geissler
R-AERO-DD	Mr. Ryan
	Mr. Buchanan
R-TEST-DIR	Mr. Heimburg
R-TEST-C	Mr. Grafton
R-TEST-CT	Mr. Perry
	Mr. Goetz
	Mr. Stone
R-TEST-I	Dr. Sieber
R-P&VE-DIR	Dr. Lucas
	Mr. Hellebrand
R-P&VE-A	Mr. Goerner
R-P&VE-P	Mr. Paul
	Mr. Isbell
	Mr. Wood
R-P&VE-PE	Dr. Head
R-P&VE-PP	Mr. Beduerftig
	Mr. Swalley
R-P&VE-PM	Mr. Fuhrmann
R-P&VE-PT	Mr. Hopson (3)
	Mr. Worlund
	Mr. Hastings (10)
	Mr. Vaniman
R-P&VE-RM	Miss Scott
PAT	
I-RM-M	
MS-H	
MS-IP	
MS-IL (8)	
MS-T (6)	

Scientific and Technical Information Facility (25)
Attn: NASA Representative (S-AK/RKT)
P. O. Box 33
College Park, Maryland 20740

DISTRIBUTION (Concluded)

Brown Engineering, A Teledyne Company
Huntsville, Alabama

Mr. Maier, MS-166

Mr. Payne, MS-190

Chrysler Corporation, Space Division
Huntsville, Alabama

Mr. Toole

Mr. Kavanaugh

McDonnell Douglas Corporation

MDC - Huntsville, Alabama

Bldg. 4481

Attn: Mr. S. L. Zukerman (3)

Lewis Research Center

21000 Brook Park Road

Cleveland, Ohio 44135

Attn: Mr. E. Otto

Mr. D. Petrash

Manned Spacecraft Center

NASA

Houston, Texas 77058

Attn: J. C. Thibodaux, Chief

Propulsion and Power Division

General Dynamics

P. O. Box 1128

Sandiego, California 92112

Attn: R. E. Tatro

Mail Zone: 584-00

Martin - Marietta Corporation

Denver, Colorado 80201

Attn: Mr. Howard Paynter

Propulsion Research Department

NASA Headquarters

600 Independence Ave., S. W.

Washington, D. C. 20546

Attn: Mr. J. A. Suddreth (3)

Code RPL

Liquid Propulsion Technology